REPORT DOCUMENTATION PAGE

Form Approved
OMB No. 0704-0188

1. REPORT DATE *(DD-MM-YYYY)*	2. REPORT DATE	3. DATES COVERED *(From - To)*
7/19/02	Final Report	10/1/99 - 3/31/02

4. TITLE AND SUBTITLE
Evaluation of NOGAPS Forcing Data

5a. CONTRACT NUMBER

5b. GRANT NUMBER
N00014-1-0073

5c. PROGRAM ELEMENT NUMBER

6. AUTHOR(S)
Axel J. Schweiger

5d. PROJECT NUMBER

5e. TASK NUMBER

5f. WORK UNIT NUMBER

7. PERFORMING ORGANIZATION NAME(S) AND ADDRESS(ES)
University of Washington
Applied Physics Laboratory, Polar Science Center
Box 355640
Seattle, WA 98105-6698

8. PERFORMING ORGANIZATION REPORT NUMBER

9. SPONSORING/MONITORING AGENCY NAME(S) AND ADDRESS(ES)
Office of Naval Research
Ballston Centre Tower One
800 North Quincy Street
Arlington, VA 22217-5660

10. SPONSOR/MONITOR'S ACRONYM(S)
ONR

11. SPONSORING/MONITORING AGENCY REPORT NUMBER

12. DISTRIBUTION AVAILABILITY STATEMENT
distribution is unlimited

DISTRIBUTION STATEMENT A
Approved for Public Release
Distribution Unlimited

13. SUPPLEMENTARY NOTES

14. ABSTRACT

Operational requirements dictate the use of NOGAPS forcing fields for the PIPS ice forecasting system. This study provides an assessment of the NOGAPS model output as a suitable source for atmospheric forcing fields for PIPS 3.0. Included in the study is an assessment of the errors in some of the most critical model variables.

20020725 043

15. SUBJECT TERMS
PIPS, longwave fluxes, shortwave fluxes, sea ice model, wind stress, surface pressure, IABP, NOGAPS, ECMWF, SHEBA, NCEP

16. SECURITY CLASSIFICATION OF:			17. LIMITATION OF ABSTRACT	18. NUMBER OF PAGES	19a. NAME OF RESPONSIBLE PERSON
a. REPORT	b. ABSTRACT	c. THIS PAGE			Axel J. Schweiger
U	U	U	UU	1	19b. TELEPONE NUMBER *(Include area code)* 206-543-1312

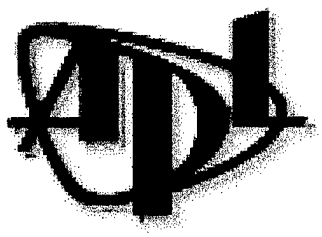

Applied Physics Laborartory
University of Washington

Evaluation of NOGAPS forcing data for PIPS 3.0

Final report on the evaluation of NOGAPS model output for the forcing of PIPS 3.0

ONR Grant: N00014-00-1-0073

Axel J. Schweiger

Applied Physics Laboratory
Polar Science Center
University of Washington
axel@apl.washington.edu

July 19, 2002

Table of Contents

Introduction

Forecasts of ice thickness and ice extent based on ice-model results are highly sensitive to the atmospheric forcing fields with which these models are driven and initialized (Fischer and Lemke, 1994; Rothrock and Zhang, 1996). Atmospheric forcing fields commonly include: Surface wind or wind stress, downwelling short and longwave radiation, surface temperature and humidity. In specifying atmospheric forcing fields, ice-modelers have a variety of choices: Output from numerical weather or climate analysis models such as NCEP, ECMWF or NOGAPS is frequently used. Climatologies for some of the variables are also a frequent choice. When making their choices model developers or operators often have little guidance assessing the quality of the forcing fields. Furthermore the impact of the errors in the forcing fields on the model output receives little attention because model parameters are frequently tuned to remove obvious biases. Progress towards better physics and more observationally constrained parameters in models requires more accurate forcing fields.

Operational requirements dictate the use of NOGAPS forcing fields for the PIPS ice forecasting system. This study provides an assessment of the NOGAPS model output as a suitable source for atmospheric forcing fields for PIPS 3.0. Included in this study is an assessment of the errors in some of the most critical model variables.

Data and Methodology

The following data sets and models were used for the evaluation of NOGAPS forcing variables:

International Arctic Buoy Program data (IABP)

This data set provides gridded daily surface temperature and surface pressure derived from drifting buoys and measurement stations as well as land stations around the Arctic. Point measurements are interpolated to grid points using an optimal interpolation scheme based on empirical autocorrelation functions. This data set has been widely used in various polar research applications and errors are estimated to be less than (2K) for temperature and < 1mb for pressure. (Rigor et al. 2000).

Navy Operational Global Atmospheric Prediction System (NOGAPS)

NOGAPS data were provided by collaborators Preller and Posey (NRL, Stennis Space Center) for the period 1997 to 2001. Twelve-hourly data were averaged and regridded into our analysis grid (EASE grid, Armstrong et al. 1995). In contrast to the comparison model data sets (see ECMWF and NCEP below), NOGAPS is not a "frozen" model but varies over time as the model is tuned and improvements in parameterizations are made. Our analysis looks at the impact of some of these changes.

National Center for Environmental Prediction (NCEP) Reanalysis Data

Data from the NCEP Reanalysis project (Kalnay et al. 1996) were obtained from NOAA Climate Diagnostics Laboratory via ftp. Daily fields on the global Gaussian grids were interpolated to our analysis grid for comparison. Data from this project are available for the same period as NOGAPS data and provide a relative benchmark for the NOGAPS model.

European Center for Medium range Weather Forecasting reanalysis data (ECMWF)

Data from the ECMWF reanalysis project are available for the period 1979-1993. This data set is known as the ERA-15 data set. This data set, though not available for the same time period as the NOGAPS subset we are using for this evaluation, provides another relative benchmark for the performance of NOGAPS.

Surface Heat Budget of the Arctic Experiment (SHEBA)

Short and longwave radiation measurements made during the SHEBA experiment were used to help evaluate the uncertainty in radiative forcing variables provided by the NOGAPS model. For this analysis we used downwelling short and longwave radiation measurements from the National Oceanic and Atmospheric Administration Environmental Resource Laboratory (NOAA-ERL) 10 meter tower (Persson et al. in press).

Radiative Fluxes measured at Barrow Data

Radiative fluxes from the long term climate monitoring site were provided by Bob Stone of NOAA-ERL. The data from this site cover the period January 1992 to July 1993 and consists of hourly measurements of downwelling short and longwave fluxes as well as surface albedo, surface air temperature, cloud fraction and relative humidity.

Reference (PFLX) data set

SHEBA point measurements of radiative fluxes only allowed a very limited evaluation of NOGAPS radiative fluxes. In order to allow a basin-wide evaluation we first had to compile reference data sets of downwelling short and longwave radiation. Substantial effort went into the compilation of these data sets. Downwelling short and longwave fluxes were computed from a combination of satellite-derived cloud fractions from the TOVS Polar Pathfinder Project (Schweiger et. al. 1999: Francis and Schweiger, 2000; Schweiger et al. in press; http://psc.apl.washington.edu/pathp), IAPB surface measurements. The methodology for computing radiative fluxes is detailed in Appendix-A and validation results are presented there. This report refers to this data set as the "reference data or PFLX data set".

Standard forcing data set

The most frequently used method of specifying radiative fluxes at the surface (Rothrock et al. submitted) applies the parameterizations first used by Parkinson and Washington (1979) [Hereafter PW] in their implementation of their dynamic sea-ice model. PW used parameterizations from Zillman (1972) for SW and Idso and Jackson (1969) for LW. Because those fluxes are most commonly used, our investigation assessed their validity and their impact on sea-ice model experiments. We refer to this data set as the "standard" data set.

Sea Ice Model

In order to obtain an initial evaluation of the impact NOGAPS errors would have on the PIPS 3.0 model, a coupled ice-ocean model was configured to conduct sensitivity studies. Even though some differences exists, the model is similar enough to the concept of PIPS-3.0 so that general conclusions of the impact of errors in the NOGAPS model can be drawn.

The coupled model consists of two components: a thickness and enthalpy distribution sea-ice

model (Hibler, 1980; Flato and Hibler, 1995; Zhang and Hibler, 1997; Zhang and Rothrock, 2001) and an ocean model embedded with a mixed layer (Zhang, 1993, Zhang et al. 1998). Both models are coupled in such a way that heat, mass, and momentum are conserved. The sea-ice model supplies surface heat, salt, and momentum fluxes into the ocean model as ocean surface boundary conditions. The ocean model, in turn, aided by the mixed-layer model, supplies surface current and heat exchange information to the ice model. Table 1 shows the main characteristics of the sea-ice model. The model is configured to allow data assimilation (Zhang et al, submitted) of ice motion data from buoys and SSM/I (e.g. Kwok et al. 1998). More details can be found in Zhang et al. (2000).

Table 1: Summary of coupled ice-ocean model components

Ocean Model	Baroclinic model with an embedded mixed layer; 21 vertical levels; ice-ocean coupling (*Zhang et al.*,1998)
Ice Model	12 thickness categories each for undeformed ice, ridged ice, ice enthalpy, and snow depth (*Thorndike et al.*, 1975, *Flato and Hibler*, 1995, *Zhang and Rothrock, 2001)*
Ice Themodynamics	One snow layer and two ice layers (*Winton*, 2000)
Ice Dynamics	Viscious plastic rheology (Hibler, 1979); line successive relaxation dynamics solver (Zhang and Hibler, 1997)
Surface Forcing	Daily; surface air temperature and sea level pressure are from NCEP reanalysis (for 1948- 1978) and from IABP (for 1979-1999); geostrophic winds, downwelling radiation, and specific humidity are derived following *Parkinson and Washington* (1975)
Model Domain	Arctic Ocean, Kara, Barents, Greenland, Iceland and Norwegian seas with area of 11.0×10^6 km^2; 40 km x 40 km horizontal resolution

Results

Temperature

A comparison of NOGAPS winter temperatures (Beesley et al., 2001) with surface measurements from SHEBA demonstrated large differences. NOGAPS analysis temperatures were up to 12 K too high during the winter month. An initial analysis indicated that this was likely due to the over-prediction of cloud cover by the NOGAPS model. Even though surface temperature is not a direct input variable for PIPS 3.0, it is a good diagnosis variable which is useful for the evaluation of the NOGAPS performance. In contrast to other variables, good validation data exist.

Figure 1 shows a comparison of surface air temperatures from the NOGAPS model, the IABP program and the NCEP reanalysis data for the period January 1997-June 2001. Plotted are the differences between the NOGAPS and IABP and NCEP and IABP fields averaged for the area north of 70°. Several noteworthy conclusions can be drawn from this analysis. Wintertime surface air temperatures in the NOGAPS analysis are up to 9 K too warm in 1997 and the early part of 1998. This is consistent with the analysis of Beesley et al. (2001) who looked at data from the SHEBA

experiments. Beginning with the second part of 1998 and the winters of 1999 and 2000 surface air temperatures in the NOGAPS analysis are too low by about 2-3°K. A check of the change-log for the NOGAPS model indicates that there was an increase in the number of levels from 18 to 24 with the move from NOGAPS 3.4 to NOGAPS 4.0 in June of 1998. The fact that summer temperatures are constrained by the melting temperature of ice may be masking (temperatures are in relatively good agreement before and after the model upgrade) the impact of this change in temperature biases which becomes clearly noticeable in the Fall of 1998. It is therefore possible that the reversal in the sign of NOGAPS errors is due to this change in NOGAPS properties. An additional change in the cloud parameterization scheme in February of 2001 appears not to have impacted the biases significantly.

The comparison of NOGAPS with NCEP forecasts shows that the NCEP model has errors similar to NOGAPS in magnitude but with an opposite sign. Although these results may provide comfort to the NOGAPS developers and demonstrate the difficulty in forecasting Arctic temperatures it highlights the need for redoubled efforts to find appropriate forcing fields for PIPS runs.

From the analysis of surface temperatures averaged over the 70° - 90° domain, it would appear that starting in the fall of 1998, NOGAPS temperature analyses are much improved. However, when comparing the spatial patterns of differences between IABP and NOGAPS analyses it becomes apparent that this is not the case. Figure 2 shows the February mean monthly differences between NOGAPS and IAPB surface temperatures for 1997-2001. NOGAPS temperatures in February of 1997 and 1998 exceed IAPB temperatures by 4-16°. From February 1999 through February 2000, NOGAPS temperatures over the western Arctic sector are as much as 16 K lower than the IABP temperatures. In the eastern part of the Arctic and over land areas, temperatures are generally higher than the IABP temperatures. The temperature biases in February 2001, following the change in the cloud parameterization scheme, appear largely unchanged when compared to the preceding years.

Summary: Large differences in surface temperatures exists through 2001. Even though air temperature averages (averages over the area north of 70°) are very close to those from the IABP buoy program, large spatial differences exists. Land areas are generally too warm. Ice-covered areas too cold. Even though temperature is not a direct forcing variable, the large differences between observed and modeled temperatures provides a good indication for the likely errors to be expected in other variables. Particularly downwelling longwave fluxes.

Longwave fluxes (LW)

The impact of surface temperature errors on PIPS 3.0 direct forcing variables is likely greatest for the downwelling longwave fluxes. PIPS is driven with downwelling longwave fluxes. Since these flux data, until recently, not available, downwelling longwave fluxes are calculated from NOGAPS net longwave fluxes and surface temperatures using Stefan-Boltzman's law and an emissivity of 1.

Figure 3 shows a comparison of downwelling longwave fluxes measured at SHEBA and from NOGAPS (using the nearest grid cell). Figure 4 shows the differences between these two measurements. In winter NOGAPS downwelling fluxes exceed SHEBA measurements by approxi-

mately 50 Wm^{-2}. SHEBA summer measurements are generally in line with the NOGAPS analysis though large differences exist for individual days. Towards the end of the SHEBA period (September 1998) NOGAPS fluxes drop well below SHEBA measurements by up to 100 Wm^{-2}. This is possibly an indication of the impact of the NOGAPS model change in June of 1998 and the subsequent underestimation of surface temperatures starting in winter of 1998 as noted above in the comparison of surface temperatures. The magnitude of these differences in measured and forecast fluxes needs to be viewed in the context of the total radiation balance. Figure 5 shows the total radiation balance measured at SHEBA. Except during the summer month the total net radiation balance is quite small (mostly negative, i.e. a loss of heat from the ice surface). A comparison of figures 4 and 5 demonstrates the severity of the problem. NOGAPS analysis errors are much larger (up to 2500%) than the net radiation balance. Since ice growth is very sensitive to the individual components of the energy balance, such a large error will undoubtedly affect the ice forecast provided by PIPS.

Shortwave fluxes (SW)

During summer SW radiative fluxes dominate the surface energy balance. Currently PIPS is driven by the net shortwave fluxes which are provided by the NOGAPS model. The reasons for this are apparently historical because NOGAPS downwelling shortwave fluxes are not readily available. We therefore compared net shortwave fluxes from SHEBA with those provided by the NOGAPS model. Figures 6 and 7 show the SHEBA measurements versus the NOGAPS analysis for the same period. NOGAPS net shortwave fluxes generally exceed measured fluxes except for July. The overestimation of SW fluxes is particularly large in May. It is important to note that there are problems associated with comparing a point measurement from the SHEBA experiment with one from a forecast model such as NOGAPS which provides an average measurement over a grid cell. This is particularly true for net shortwave fluxes since the net fluxes are computed from the differences of downwelling and upwelling SW fluxes. Upwelling fluxes are of course subject to large inhomogeneities of the surface (e.g. melt ponds) and their effect on the surface albedo. However, during spring before melt, the surface is still rather homogeneous so that the point measurements are representative at the grid cell scale.

A comparison of figure 7 with 5 (net) again shows that the differences between NOGAPS and SHEBA -a measure of the uncertainty in the NOGAPS analysis- are several times greater than the net radiation balance. This again indicates that the PIPS ice forecasts are likely to be severely impacted by the errors in NOGAPS SW fluxes. Errors in NOGAPS net fluxes are a combination of errors in the computation of downwelling fluxes and surface albedo within the model. A comparison of these individual components would be more useful with respect to finding the sources of error, but the comparison of net fluxes which are used for driving the PIPS model provides an assessment of the potential impact of these errors on PIPS forecasts.

Comparison of cloud cover

It is difficult to identify the source of errors in the NOGAPS forecasts of downwelling radiation. However, since clouds significantly modify the downwelling radiative fluxes, it is important to investigate the total cloud cover computed by the NOGAPS model with cloud cover observed at SHEBA (Figure 5). Excess cloud cover is present in the NOGAPS analysis during the winter month. This was noted previous by Beesley (2001) as the likely principal cause for the up to 9K

overestimation of surface temperature by NOGAPS during the winter of 1997. However, a time series (Figure 9) of total cloud cover from October 1997 through December of 2000 does not indicate a substantial change in the cloud cover regime after 1998 when temperature analyses changed dramatically in NOGAPS.

During May when the largest differences occur between downwelling shortwave fluxes measured at SHEBA and those produced by the NOGAPS model, differences in cloud cover are actually rather small (~10%). This leaves cloud optical properties or surface albedo as analyzed by the NOGAPS model as the potential sources for the large observed differences in net shortwave radiation.

Recommendation: Future work should examine the surface albedo produced by NOGAPS and the downwelling fluxes separately in order to untangle errors due to the parameterization of albedo versus the representation of clouds and their effect on the shortwave fluxes in the NOGAPS model. PIPS also should move towards using downwelling shortwave fluxes rather than NET fluxes from NOGAPS. Without significant additional computational overhead the PIPS model should be able to predict surface albedo as a function of snow and sea ice conditions. Parameterization for surface albedo are part of the thickness distribution model (Bitz et al.) being adopted for PIPS 3.0. Although not perfect, the resulting surface albedo is likely to be better than those obtained by NOGAPS with its much simpler sea ice formulation. Using downwelling rather than net shortwave fluxes would allow changes in sea ice cover as predicted by PIPS and their effect on the surface albedo to have a direct impact on ice predictions. Given the importance of the surface radiation balance, this strategy appears to be a better than relying on the accuracy of net shortwave fluxes provided by the NOGAPS model.

Comparison of shortwave fluxes from NCEP and ECMWF

In order to put NOGAPS SW errors in perspective this study compared downwelling shortwave fluxes from the NCEP and ECWMF reanalysis data sets with our reference data set (PFLX) which was computed from TOVS cloud fractions. Figure 10 shows differences between each of the reanalysis outputs with the PFLX data set averaged over the area north of 60°N for 1990. The results show that the NCEP reanalysis has errors of similar or greater magnitude than the NOGAPS forecasts. The ECMWF appears to significantly underestimate SW fluxes during spring (March, April, May) but performs rather well during the rest of the year. This analysis shows that problems in forecasting downwelling shortwave radiation are not unique to the NOGAPS model. In light of the rather good performance of the ECMWF model, future improvements in NOGAPS could achieve a similar or better performance.

Model Sensitivities

This section we study analyzes what the impact of errors in NOGAPS radiative forcing fields have on the sea ice model. Sensitivity studies were conducted with a coupled ice ocean model (described below). A sample of the results is presented below.

Sensitivity of model output to errors in longwave forcing fields?

In order to test the sensitivity of the model parameters to errors in the forcing fields we conducted several model experiments. The coupled ice-ocean model discussed above is driven alternatively

with longwave fluxes obtained from NOGAPS (using NET LW and surface temperature see section on data and methodology) and with net-fluxes from the standard data set (CONTROL). Figure 11 shows the mean difference in ice thickness from the two experiments. Ice thicknesses computed using the NOGAPS longwave forcings are mostly smaller because of the overestimation of downwelling longwave fluxes associated with temperatures that are too high. Greatest differences in ice thickness are in the western Arctic in the order of 0.5 to 1 m with extreme values in the 1-2 m range near the Canadian Archipelago.

Sensitivity of model output to errors in SW forcing fields

In order to obtain a sense of the potential impact of errors in the SW fluxes provided by the NOGAPS model we conducted the following experiment. Since NOGAPS only provides net shortwave fluxes, we first had to compute downwelling fluxes. We did this by using the albedos generated by the sea ice model (during the control run) to compute downwelling shortwave fluxes from the net SW fluxes provided by the NOGAPS model [S=net(1-alpha)]. As discussed earlier, downwelling shortwave fluxes calculated in this manner are subject to errors in atmospheric properties (clouds) produced by NOGAPS and to differences in surface albedo computed in the sea ice model versus the assumptions for ice albedo in NOGAPS. Thus results in figure 12 only provide a sense of the potential sensitivity due to shortwave errors. Figure 12 shows the results for September 1998. (Sensitivity is greatest at the end of summer). Mean ice thickness computed using NOGAPS derived shortwave fluxes is 1-2 m less than for the reference data set. This example illustrates how biases in SW fluxes are capable of producing rather unrealistic results.

Do shortwave fluxes really matter ?

The analysis in the previous section has shown that errors (biases) in shortwave fluxes can have a dramatic impact on sea ice model output. Because of the strong sensitivity to SW flux errors and the poor performance of NOGAPS in this area, we nex investigated ways to minimize the problem. As an alternative to using NOGAPS produced radiative fluxes, would be to use climatological values for downwelling SW. (Output from a different model, e.g. ECMWF, is not an option because of operational constraints). In order to investigate the need for time-varying forcing SW forcings fields over a climatology we conducted two model experiments: 1) The coupled ice-ocean model was run with the daily varying SW fluxes from our reference data set (PFLX), and 2) the model was run with a climatology of SW fluxes generated by averaging daily fluxes of the 18 years (1980-1998) for our reference data set period. Figure 13 shows the standard deviation of the difference in ice thickness using the climatological SW forcings vs. daily varying SW forcings for September. This difference is a measure of the ice thickness variability due to inter annual variations in SW fluxes. As apparent from Figure. 13 this variability is rather small with a standard deviation of 8-10 cm ice thickness (Figure 14) Figure 14 shows the standard deviation of ice thickness during September for this period. Values are in the order of 80 cm. A comparison of Figures 14 and 13 indicates that the variability in ice thickness due to variations in SW fluxes is actually rather small and in the order of 10-15%.

Recommendation

Given the large potential impact of "unpredictable" errors in the SW fluxes as produced by NOGAPS and the relatively low variability associated with this variable, it would seem reason-

able to employ climatology for model runs rather than NOGAPS output. In other words: A good climatology might yield better results than a poor model, particularly if the variability is low.

Surface pressure

A comparison of surface pressure from the NOGAPS analysis with surface pressures from the NCEP analysis (Figure 15) shows minimal differences. Since observations of surface pressure from land stations and drifting buoys are assimilated in both models, this is not too surprising. Because observations were assimilated into these analyses, surface pressures are likely a high quality variable.

Wind stress

A large fraction of the variability in sea ice thickness is associated with the variability in the surface winds and the resulting stresses (Zhang and Rothrock, pers. comm.). The large errors in surface temperature observed in the NOGAPS analysis raise the question of whether the boundary layer structure over sea ice is appropriately modelled by the NOGAPS model. Any errors in the boundary layer temperatures are likely to have a significant impact on the surface wind stress calculated by the NOGAPS model. Wind stresses from NOGAPS are in turn used by PIPS as one of the principal forcing fields. Traditionally sea-ice models are driven with surface stresses computed using geostrophic winds and fixed or seasonally varying coefficients for the air/ice drag (Ip 1993) according to $\tau=\rho C_g G^2$, where τ is the surface stress, ρ the air density, C_g the geopstrophic drag coefficeint and G the geostrophic wind speed. In order to assess the quality of the NOGAPS surface stresses we again conducted two separate model experiments. In the first experiment we used the surface pressure from the IABP buoy program and seasonally varying drag coefficients following Ip (1993) to compute surface stresses. The second experiment, we used surface stresses provided by the NOGAPS analysis. Daily ice motion from these model experiments was then correlated with observed buoy motions. Table 2. shows the results from these experiments. With respect to ice velocities the sea ice model apparently performs better when driven with NOGAPS surfaces stresses than when the stresses are computed from the surface pressure. During summer 12% additional variance in daily ice velocities are explained when using NOGAPS stresses. In winter when NOGAPS surface temperature analysis have large errors, NOGAPS stresses still improve model ice velocities by 8% in explained variance. Fig 16 shows the spatial distribution of the squared correlations and indicates that the superior performance of the model driven with NOGAP stresses is fairly evenly distributed with some concentration in the Beaufort Sea area. Interestingly, a comparison of buoy correlations with model experiments using IABP surface pressures and NCEP surface pressures yields a very similar difference as observed in the IABP, NOGAPS stress comparison. This result indicates that the NCEP and NOGAPS surface pressures are superior to those from the buoy program. Noting the fact that there are only very small differences between NOGAPS and NCEP surface pressures, it is likely that most of the additional explained variance in ice velocities (when using NOGAPS) comes from the better pressure field in the NOGAPS data and that the calculation of surface stresses yields little skill in terms of the prediction of ice velocities. A direct comparison of buoy correlations using NOGAPS surface pressures vs. NOGAPS surface stresses would have to be conducted to answer this question conclusively.

Table 2: Squared Velocity Correlations (R^2)

	NOGAPS	Surface Stress Calculated from Surface Pressure
Winter	.43	0.35
Summer	0.59	0.468
Allyear	0.46	0.41

Table 2. Correlations of daily buoy velocities with model velocities. Squared correlations are shown. Data are for approximately 8,000 daily observations for 1997 through 1998

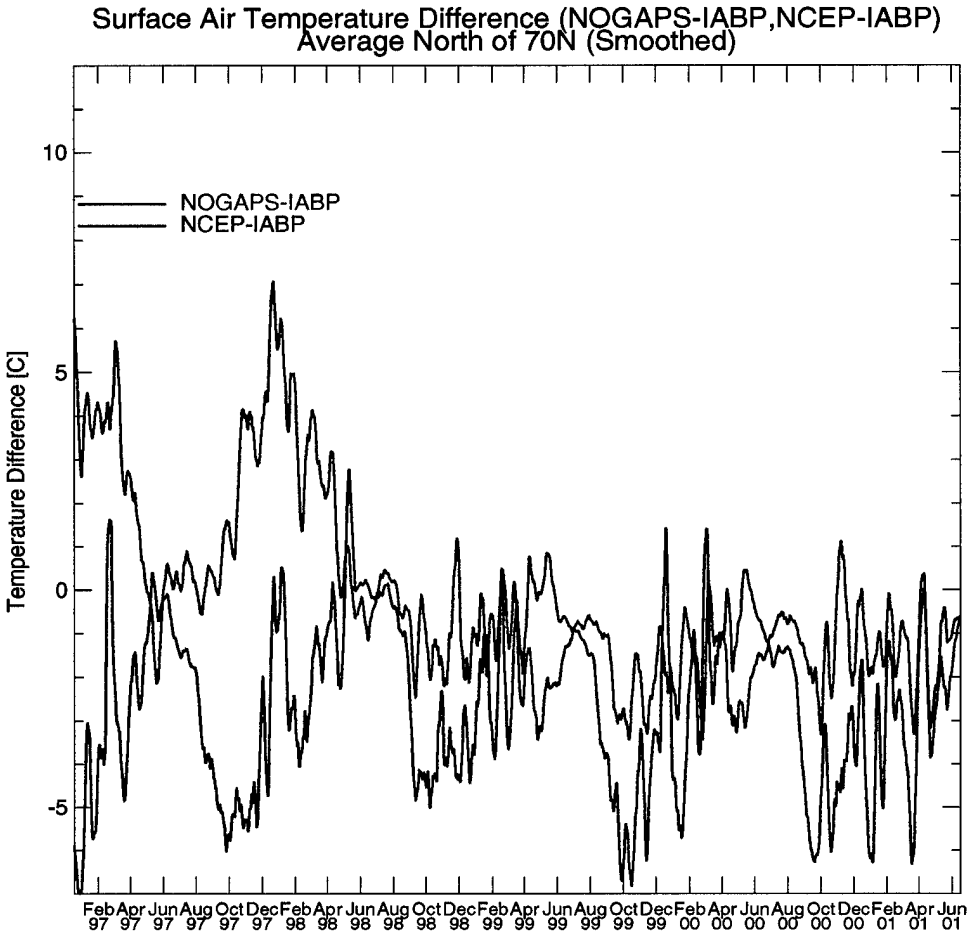

Figure 1: Difference in surface air temperature between the NOGAPS analysis and the IABP buoy data set and the NCEP reanalysis and the buoy data set. Data are 10-day running mean.

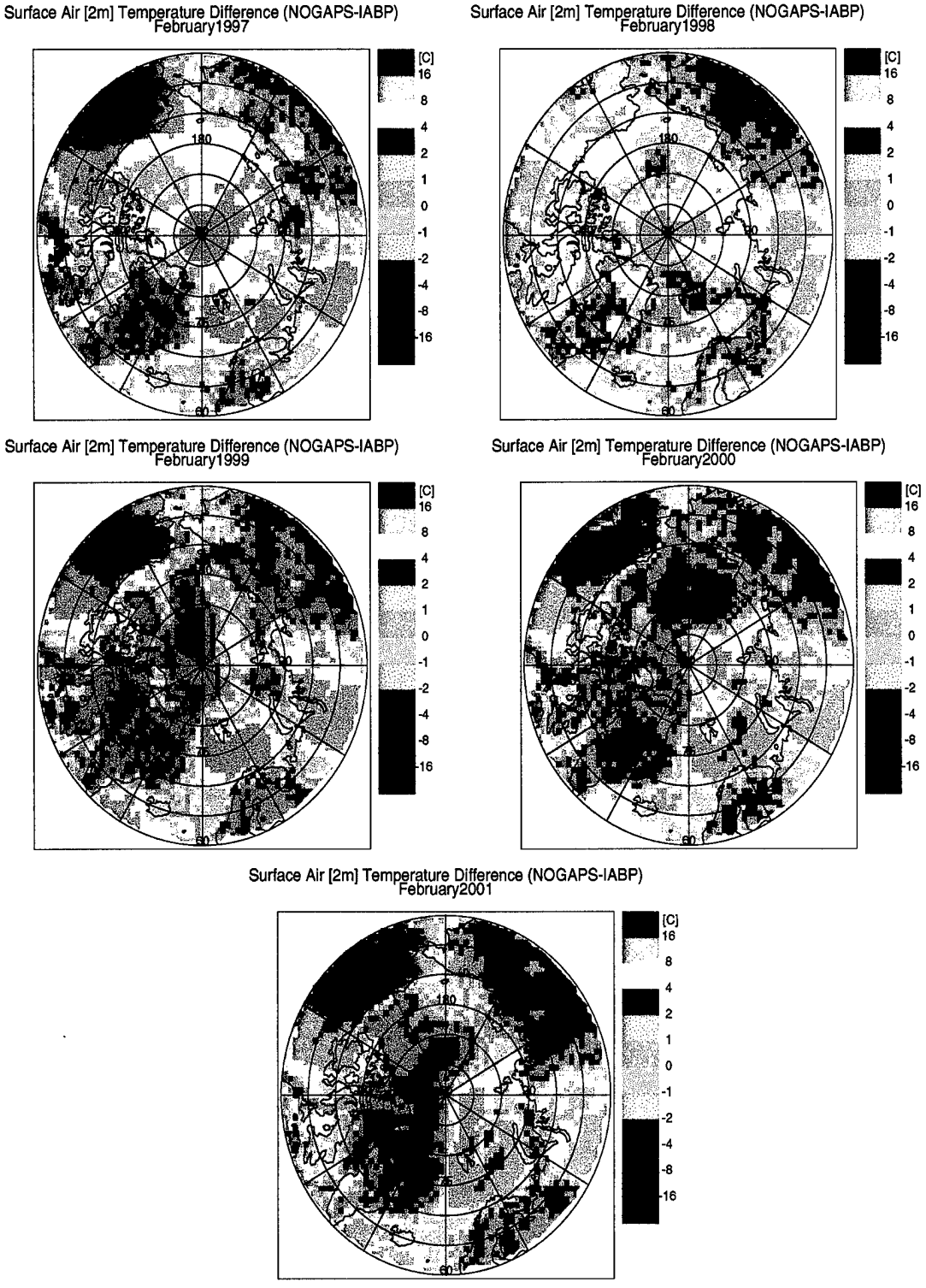

Figure 2: Difference in mean monthly surface air-temperture from the IABP program and the NOGAPS analysis. (NOGAPS-IABP) for February 1997-2001

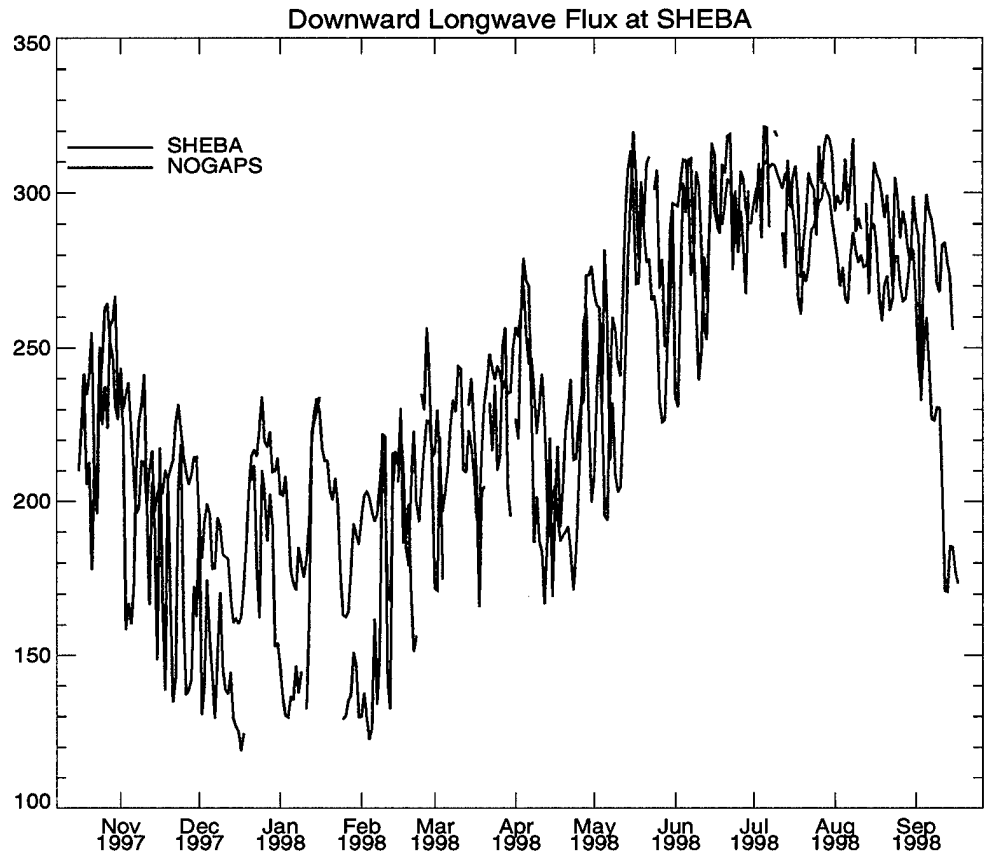

Figure 3: Downwelling longwave fluxes computed from NOGAPS net longwave fluxes and SHEBA measurements.

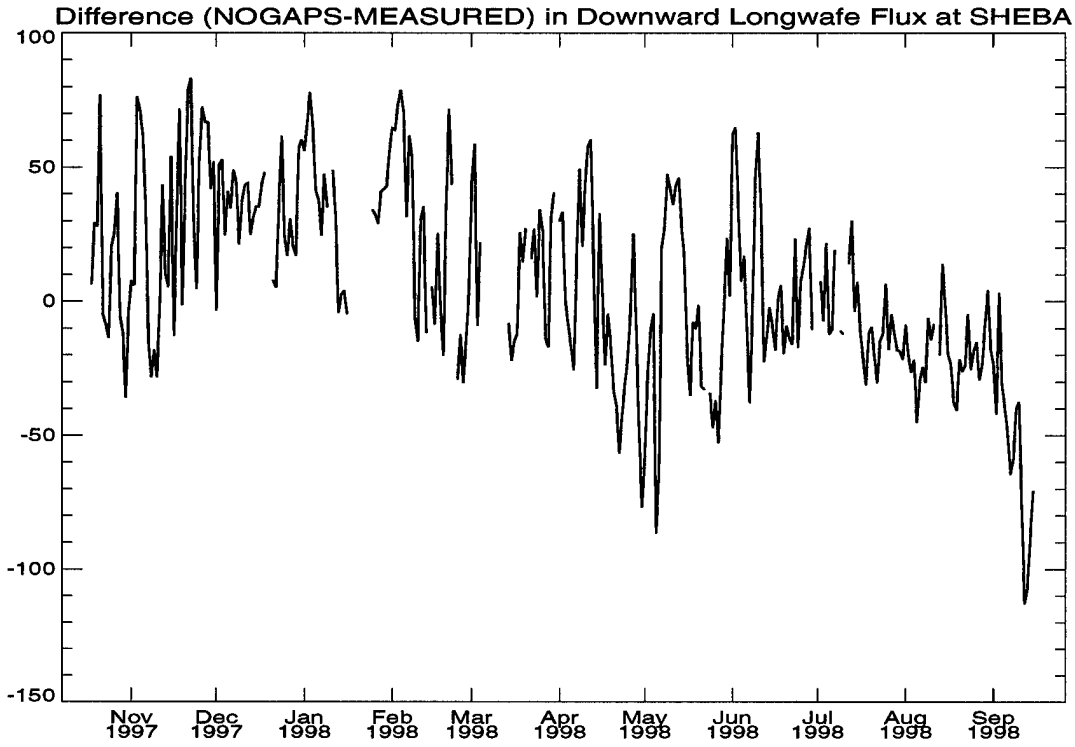

Figure 4: Differences in downwelling longwave fluxes computed from NOGAPS net longwave fluxes and SHEBA measurements.

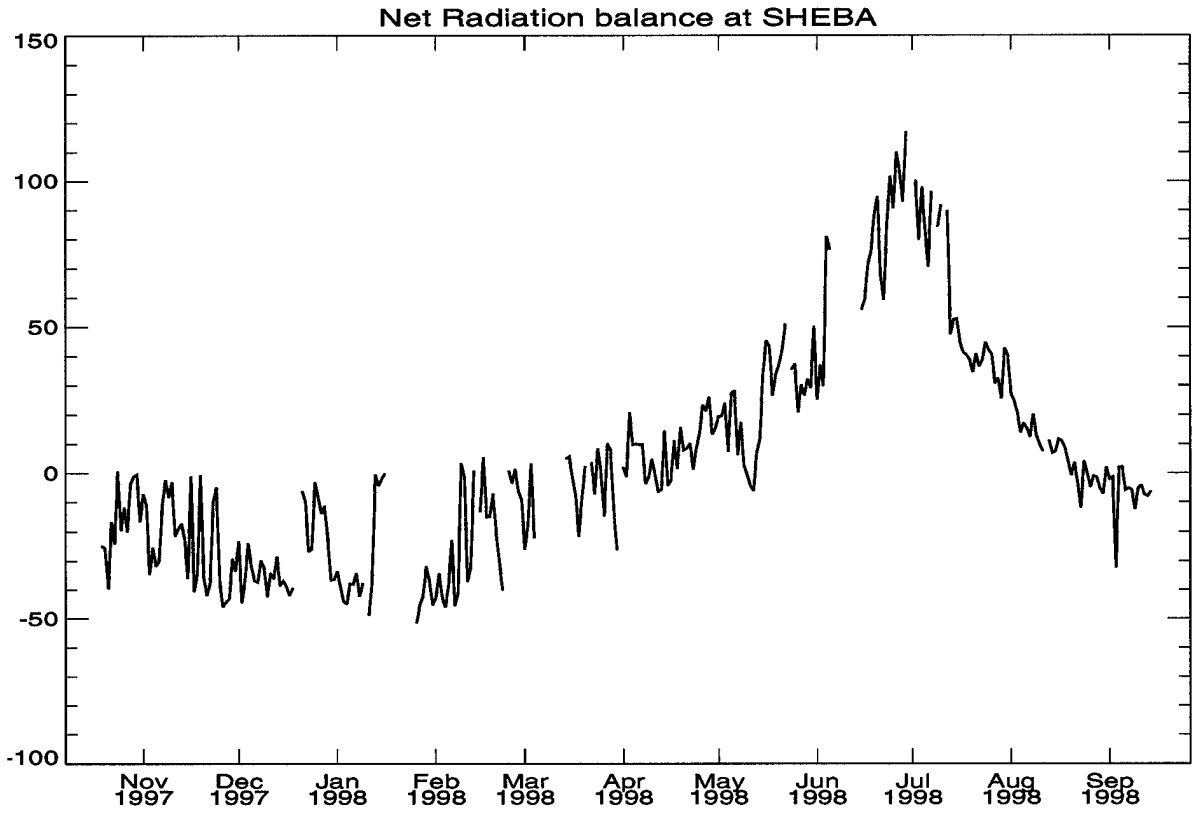

Figure 5: Net radiation balance measured at SHEBA.

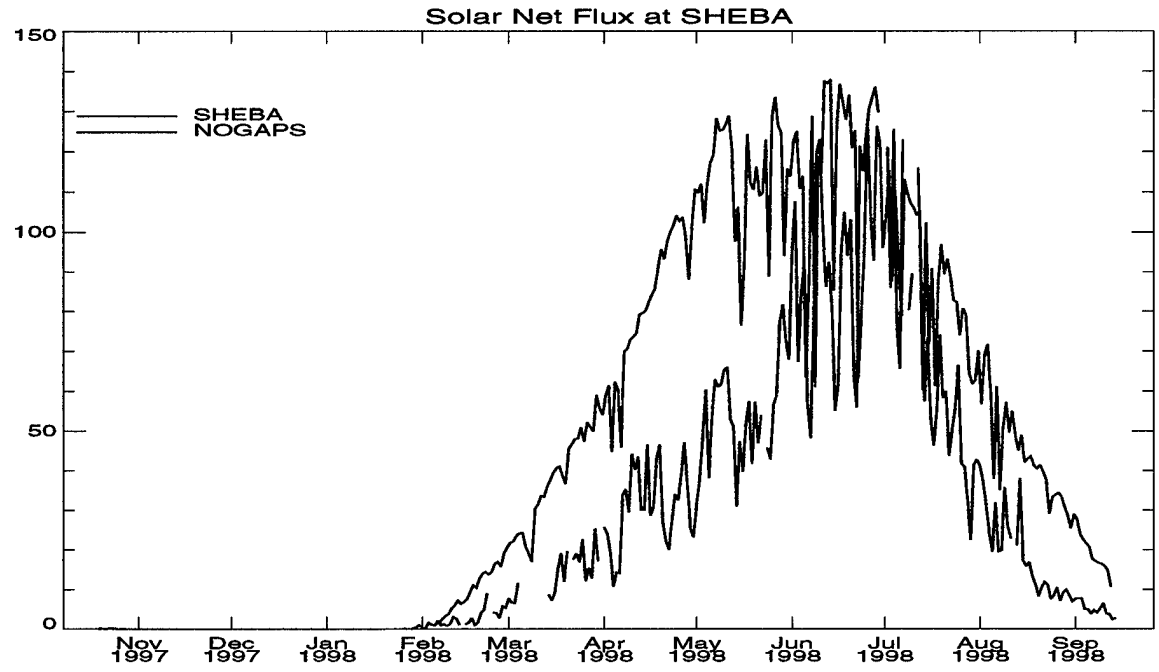

Figure 6: Net shortwave radiation balance measured at SHEBA (ERL-TOWER) and NOGAPS analysis.

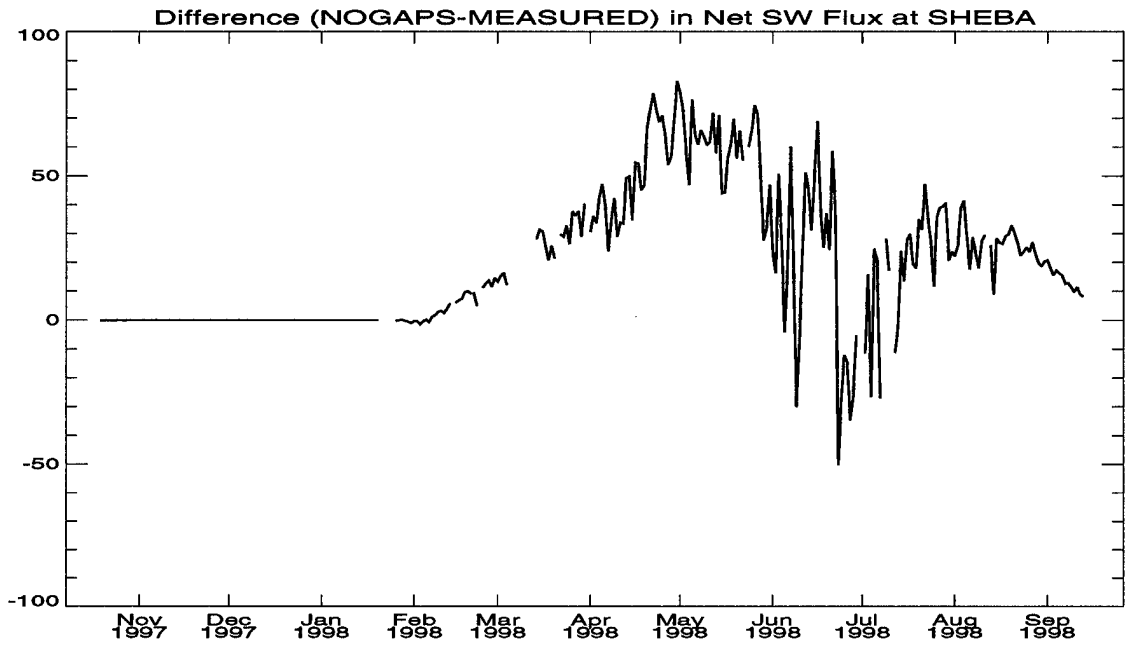

Figure 7: Difference in net shortwave radiation between SHEBA measurements and NOGAPS analysis.

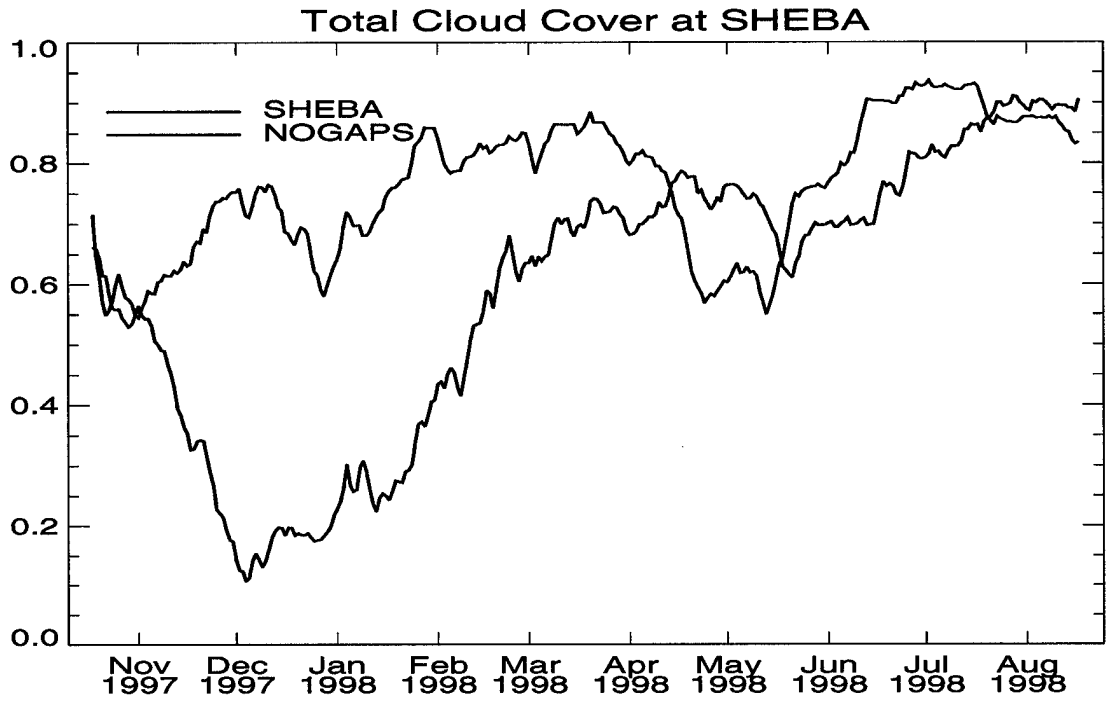

Figure 8: Total cloud cover from the NOGAPS analysis and the total cloud cover observed at SHEBA.

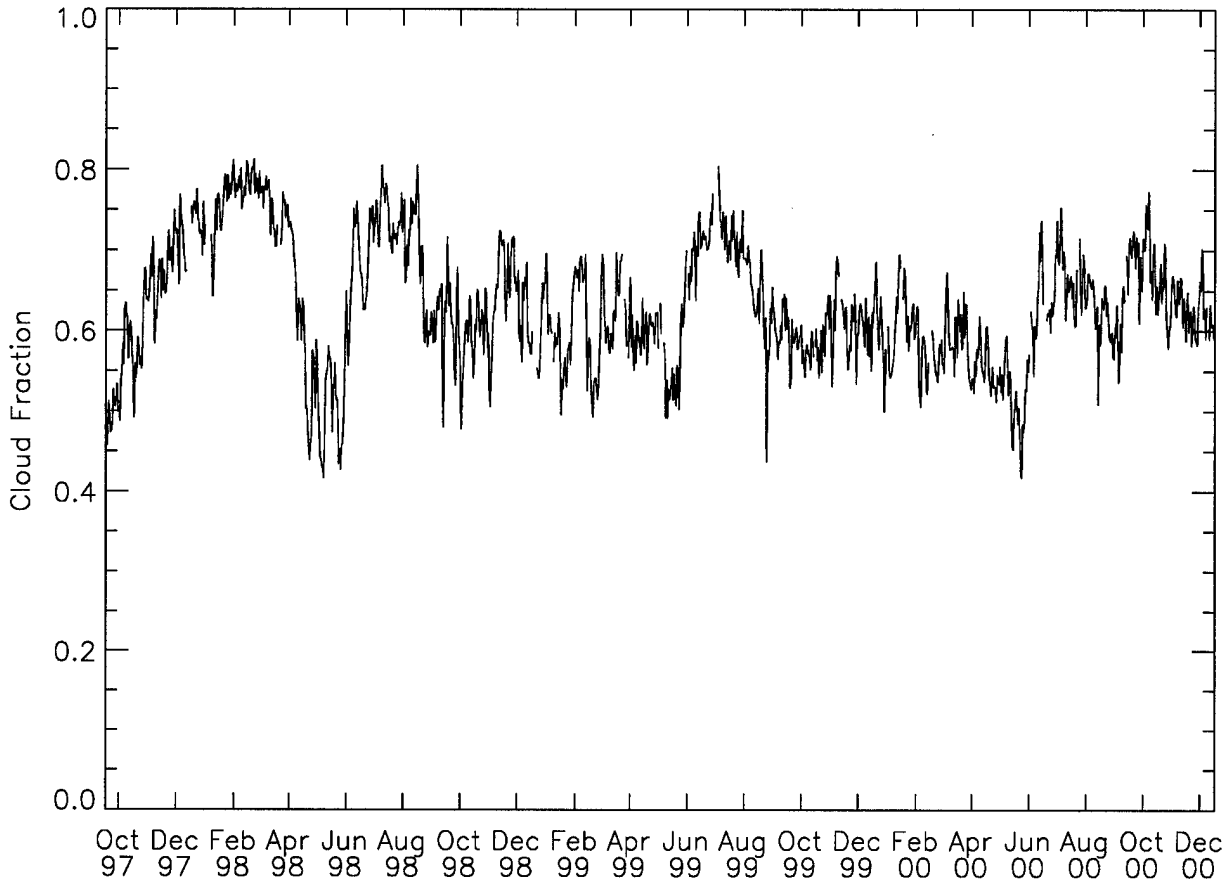

Figure 9: Total cloud cover from NOGAPS averaged for the 70 ° to 90 °N domain. The period October 1997 through December 2000 is shown.

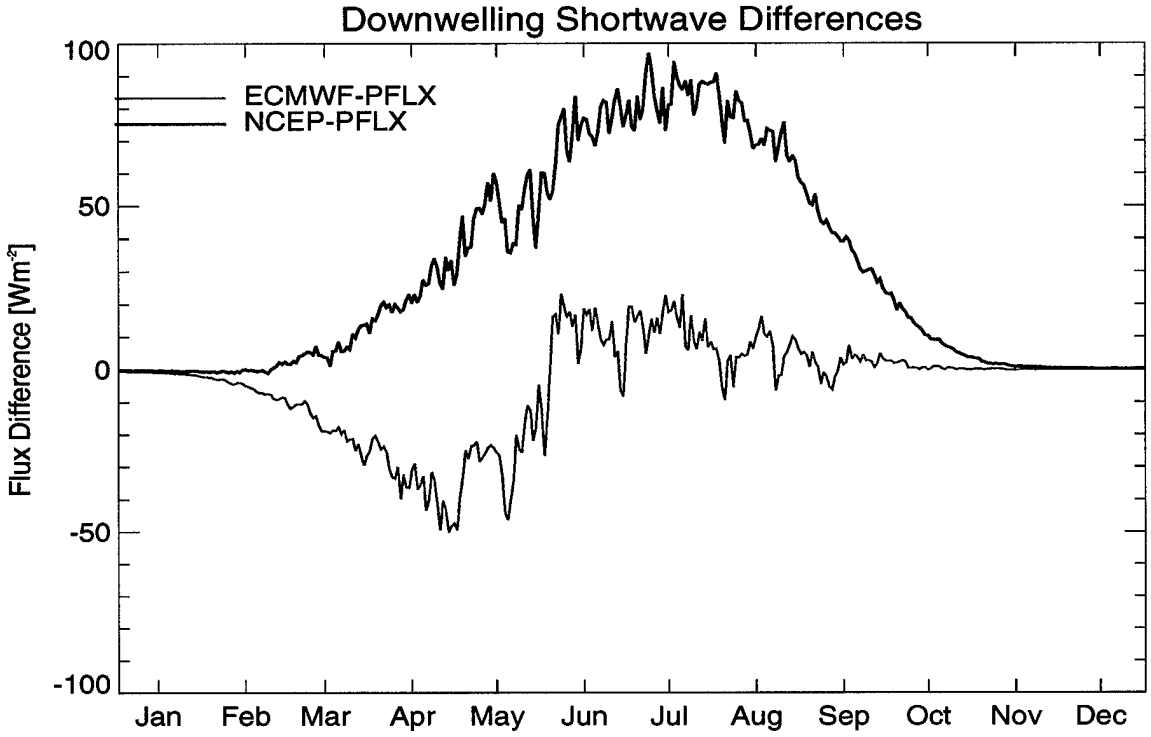

Figure 10: Comparison of downwelling shortwave fluxes from the ECMWF and NCEP Reanalysis projects. Shown are differences between each of the data sets with a reference data set (PFLX) which is derived from TOVS cloud fractions and parameterizations of surface fluxes. Averages over the area of 60° N for 1990 are shown.

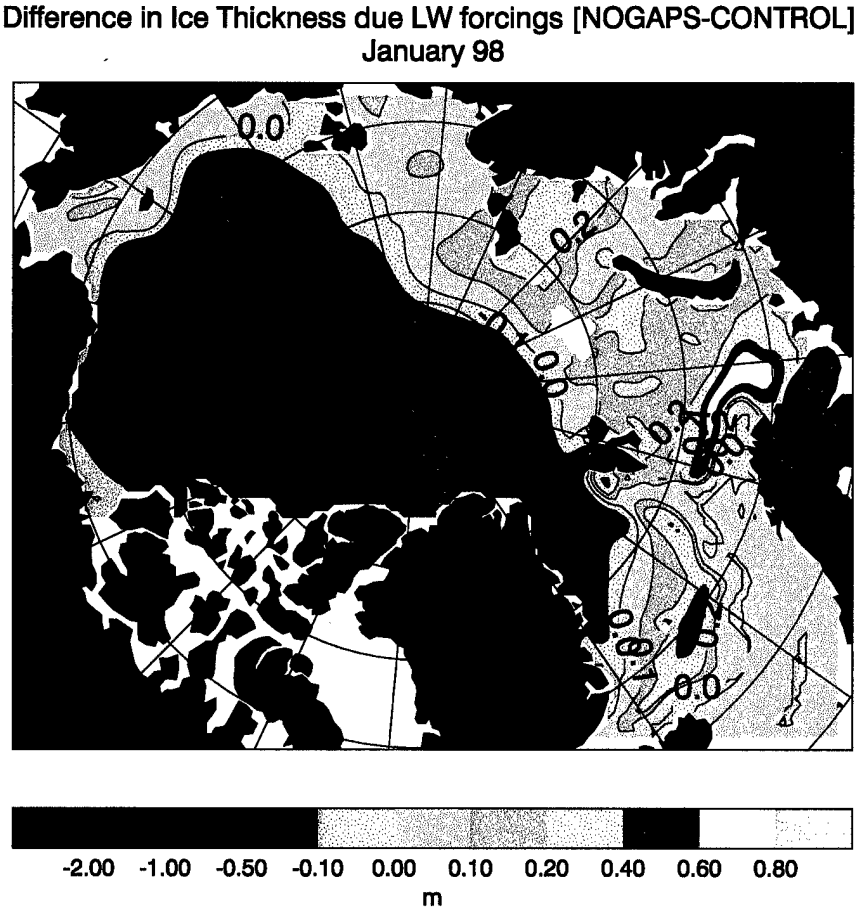

Figure 11: Difference in modelled mean ice thickness using NOGAPS LW forcings versus a reference data set based on IABP buoy temperartures. Data is for January 1998.

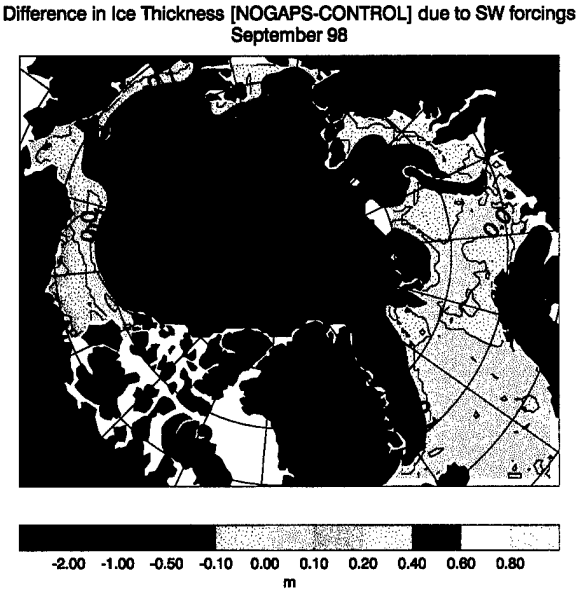

Figure 12: Difference in mean ice thickness using NOGAPS shortwave forcings versus. reference data set PFLX. Differences in ice thickness are shown for September 1998.

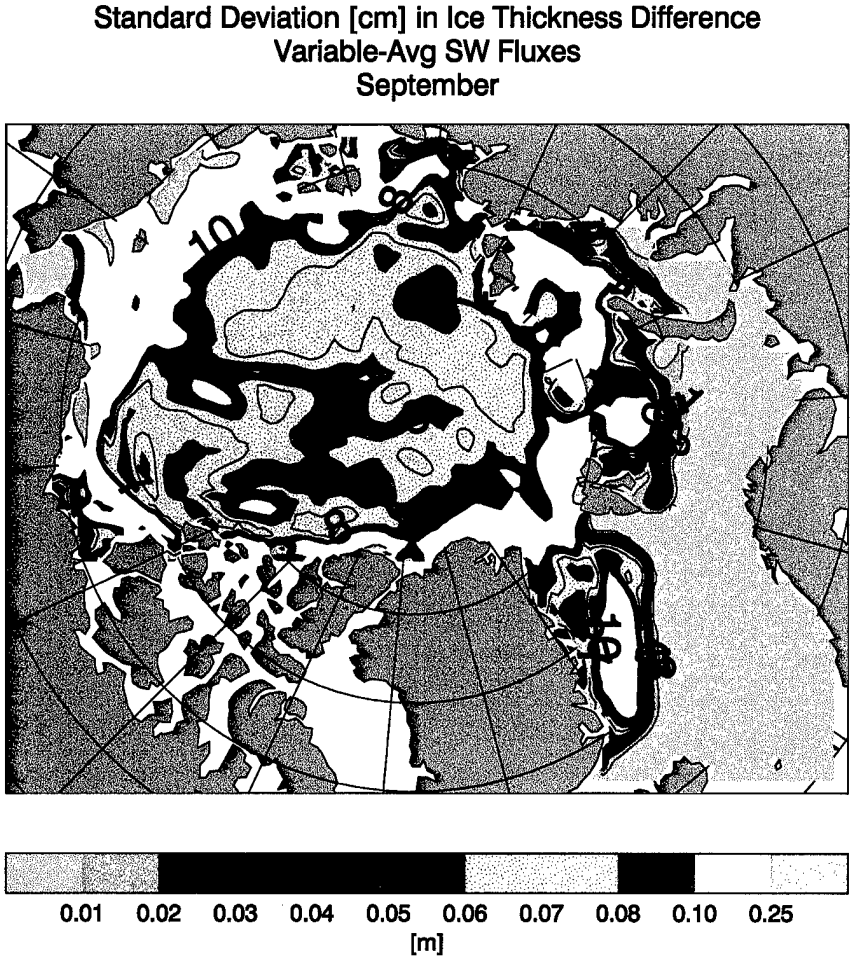

Figure 13: Standard deviation of the ice thickness difference between using daily varying and climatological SW fluxes.

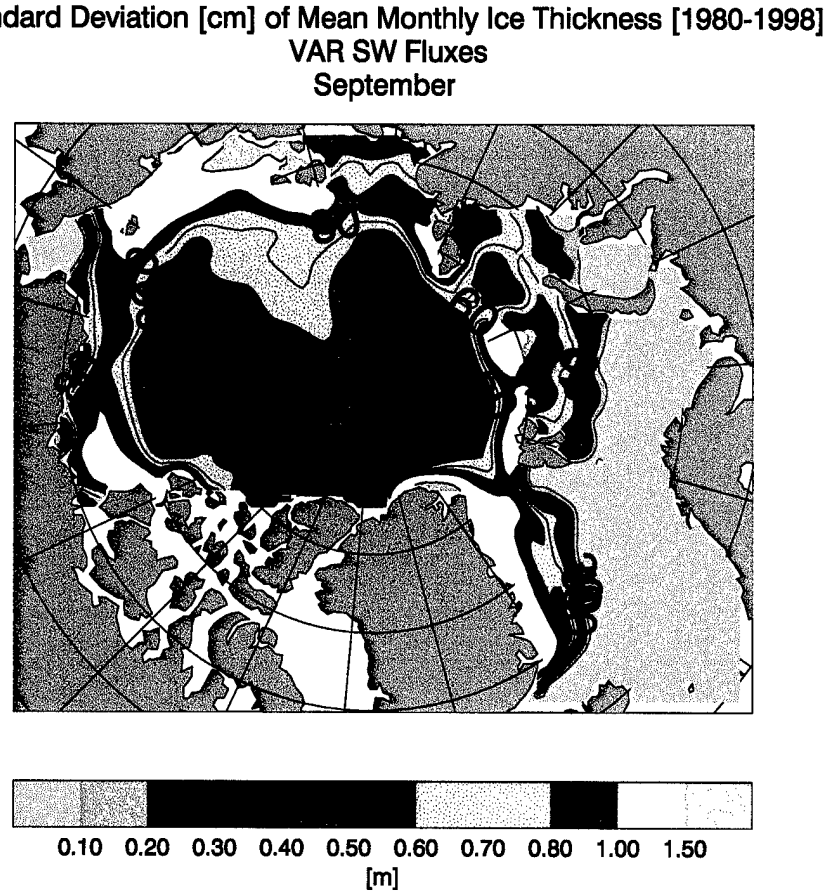

Figure 14: Standard deviation of modeled mean monthly ice thickness for the period 1980-1998.

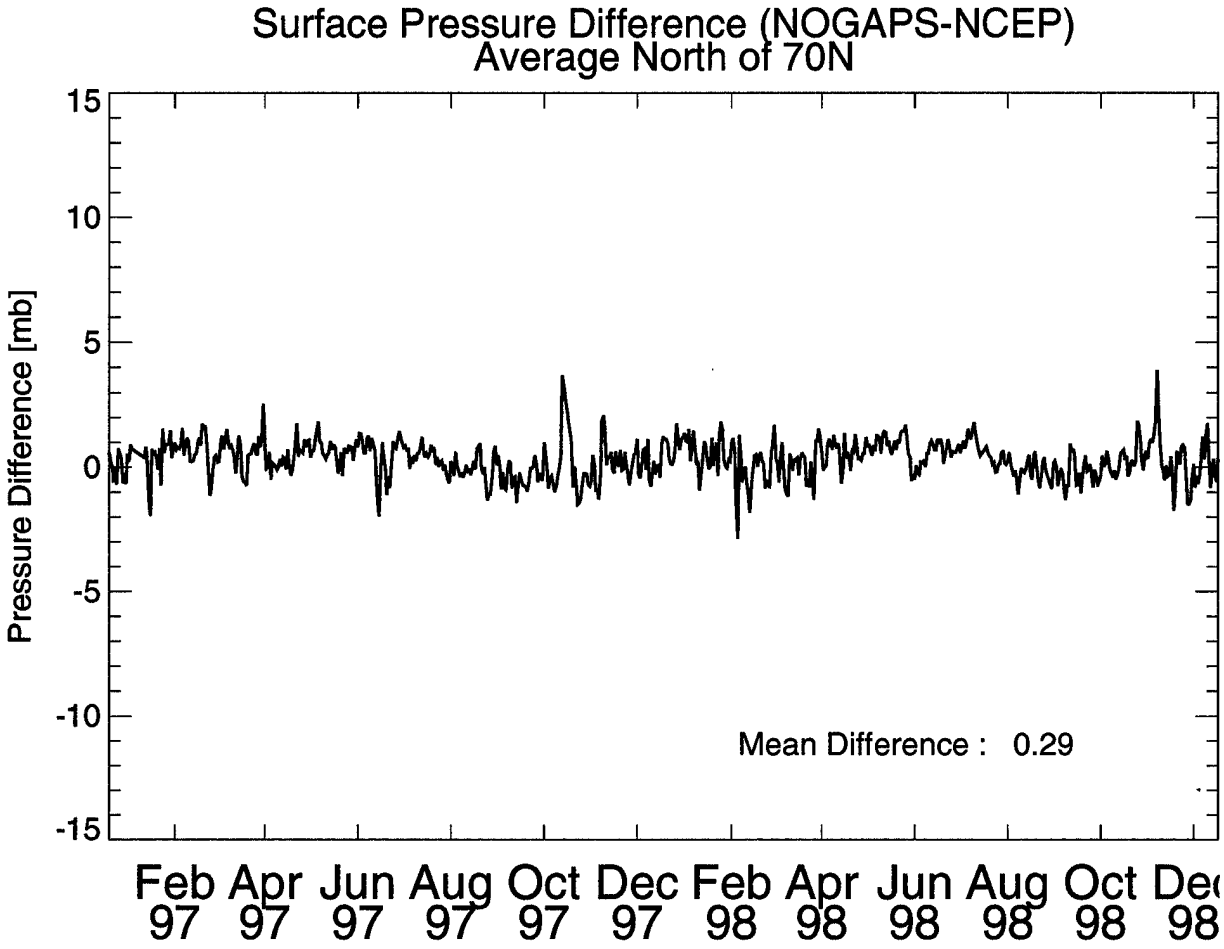

Figure 15: Sea level pressure difference between NOGAPS and NCEP analysis. Pressure averaged over 70°N.

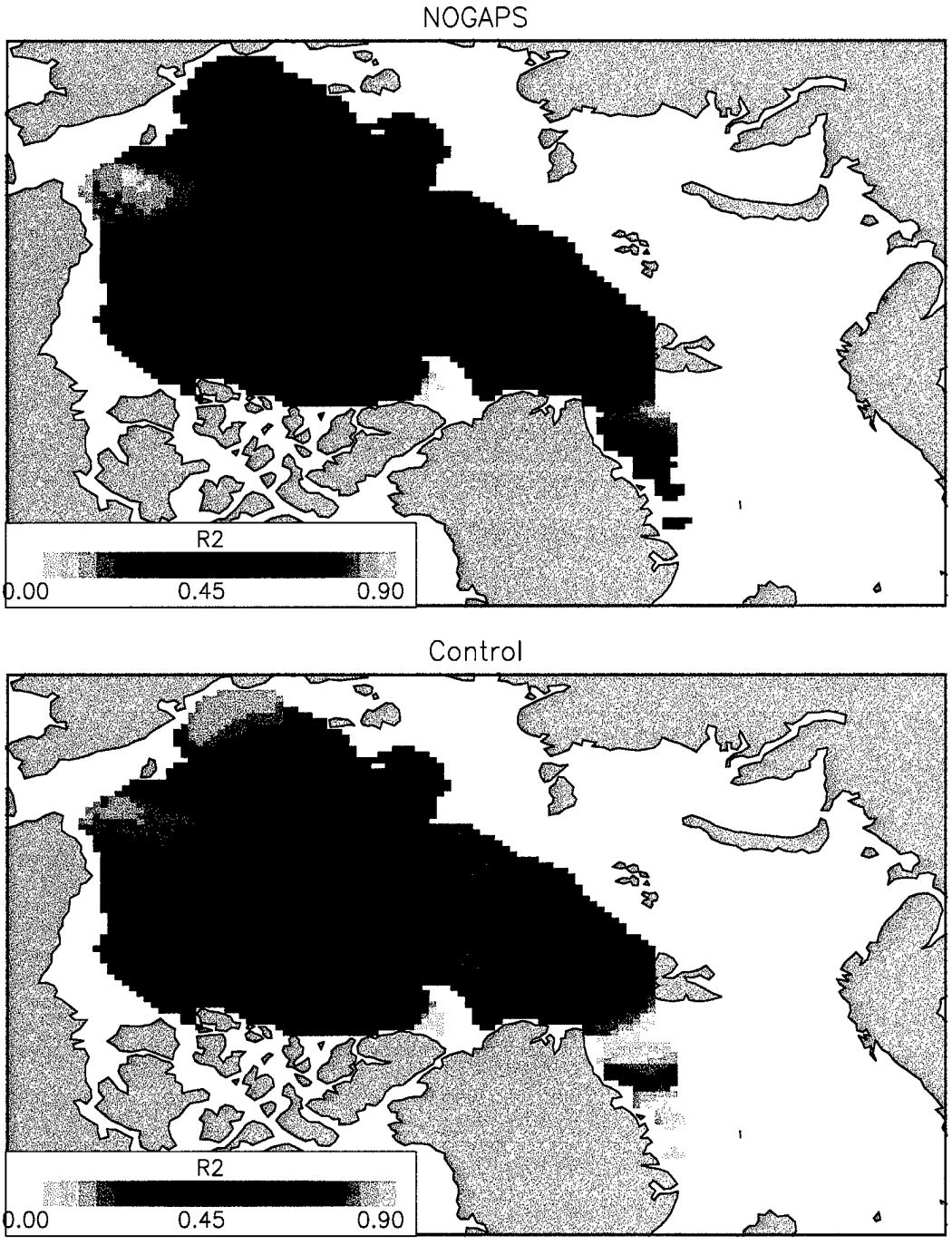

Figure 16: Correlations of modeled ice velcocities with daily buoy measurements from two experiments. a) Driving the sea-ice model with NOGAPS windstress and b) driving the model with surface stresses calculated from IABP surface pressures.

Appendix: Reference data set

Radiative forcing fields for sea ice model experiments have traditionally computed using simple parameterizations which predict downwelling long and shortwave fluxes from temperature, cloud fraction and humidity. For a review of such parameterizations see Key et al., 1996. Sources for these variables vary greatly (see review by Zhang and Rothrock, submitted). Alternatively, radiative fluxes from forecast models such as NCEP, ECMWF or NOGAPS have been used to drive sea ice models. Despite the well known sensitivity of sea ice model output due to errors in these forcing fields (Fisher and Lemke, 1994, Rothrock and Zhang, 1996), relatively little effort has gone into the validation of these fields. This is in part due to the scarcity of reliable validation data.

As shown in the main part of this report, very large differences between parameterized, forecast model and fluxes observed at the surface exists (e.g. SHEBA).

In this appendix we describe the compilation of "reference" data sets for downwelling long and shortwave fluxes for use in models of the Arctic ice/ocean system. These reference data sets attempt to provide the best possible estimate of the true forcing fields. Their purpose is twofold:

- To compare radiative forcing field from forecast models such as NOGAPS, ECMWF, and NCEP or any other source beyond a single point and create a "map" of error estimates for the respective source.
- To allow the impact of errors in forcing fields (e.g. NOGAPS) on sea ice model output.

Approach

In order to achieve a spatial and temporal coverage suitable for ice model experiments our approach seeks to compute downwelling short and longwave fluxes through a combination of satellite and surface measurements as inputs to fast and relatively simple parameterizations which have been tuned and tested for polar environments.

Downwelling shortwave fluxes (DSF)

Downwelling shortwave fluxes at the surface depend primarily on the solar zenith angle, cloud amount (fraction of the sky covered by clouds), cloud height, cloud microphysical properties (optical depth, droplet size distribution and phase), effects on aerosols and water vapor in the atmospheric column and surface albedo. Given accurate measurements of these variables, radiative transfer calculations allow the calculation of surface radiative fluxes with the help of sophisticated radiative transfer models. Unfortunately quite a few of the variables necessary to conduct radiative transfer calculations are only available for short time periods and in very few locations. However, comparisons of relatively simple parameterizations which use only a subset of these variables have been shown to achieve good results when compared to measurements and more detailed radiative transfer calculations (c.f Key and al., 1996). For DSF, the parameterization of Shine (1984) (Eq. 1) has been found provide the best results:

$$
\begin{aligned}
S_{cldy} &= \frac{53.5 + 1274.5\cos(\theta)}{(1 + 0.139(1.0 - 0.935\alpha)\tau} \\
S_{clr} &= \frac{S_o \cos(\theta)^2}{1.2\cos(\theta) + (1 + \cos(\theta) * 0.001e + 0.0445)} \\
S_{tot} &= S_{clr}(1 - C) + S_{cldy}C
\end{aligned}
\qquad (1)
$$

Where inputs for this parameterization are solar zenith angle (θ) cloud amount (C), water vapor pressure (e), surface albedo (α) and optical depth (τ).

Where will those inputs come from to allow sufficient temporal and spatial coverage. Sources selected for the compilation of the reference data set are summarized and discussed below:

Solar zenith angle

The solar zenith angle is simply calculated from latitude, longitude and time. Daily averages of DSF can be computed by integrating θ from sunrise to sunset and using the result in equation 1. The resulting flux is then weighted by the time between sunrise and sunset to obtain a daily average shortwave flux (SW)

Cloud amount

Cloud amount is the fraction of the sky obscured by clouds. This variable is part of standard meteorological observations made by human observers and is thus only available where such observations are made with regularity. From May through August, this variable explains the greatest amount of variance in DSF. Figure A-1 demonstrates the value of such "subjective" observations in quantifying DSF. A comparison of measured DSF with parameterized DSF using observed cloud fractions vs. random values shows that observed cloud fraction accounts for 64% of the variances in measured DSF. Even though a great deal of cloud amount observations of this kind are available from the record from the former Soviet Union North Pole (NP) stations (c.f. Lindsay, 1998) and from other experiments throughout the Arctic, there is an insufficient number of such stations to construct a spatially and temporally continous field. Comparisons of meteorological surface observations with cloud observations in a new data set (TOVS Path-P) obtained from satellite (Schweiger et al. 1999, Schweiger et al, in press) have demonstrated that satellite observations appear suitable to characterize the variability in cloud amount in the Arctic. We have therefore selected this data set, available as daily averages with 100 km for the Arctic north of 60° N for the years 1979-1998 to provide the input for cloud fraction (Schweiger et al., 1999, http://psc.apl.washington.edu/pathp)

Humidity

In the Arctic, because of the low temperatures, the amount of water vapor at the surface is very small and can be shown to have only a very minor influence on the DSF. Measurements at the SHEBA camp showed that relative humidities are generally 100% with respect to ice. For simplicity we therefore also assume relative humidity to be saturated with respect to ice for our DSF calculations.

Surface albedo (α)

Because of multiple scattering between a high albedo surface and low clouds, the surface albedo plays a role in the DSF received at the surface. However, an analysis of measurements at the SHEBA camp showed that only a small amount of the variance in DSF is explained by variations in the surface albedo. For the purpose of optical depth calculations (see below) and in validation of the study's approach measurements of surface albedo at the NP stations were used. Rather than using individual albedo measurements from NP stations, NP station albedos were averaged by day of year and smoothed using a 30-day running mean. *Note that this albedo is only used in the design and validation of the study's approach. In the model experiments described below, surface albedos generated by the sea ice model are used. This is done to allow interaction of surface albedo and DSF which becomes more important when sea ice is completely removed.*

Optical thickness (τ)

The parameterization of Shine (Equation 1) requires a value for cloud optical thickness (τ). Measurements from a few field experiment don't allow a temporal and spatial characterization of this variable. However, a wide range of measurements of DSF are available from the NP stations. Following the approach of Lindsay (1998) we therefore solve equation (1) for τ then, given a cloud fraction (c), surface albedo (α) and vapor pressure, we can compute τ for each set of observations. The optical thickness calculated in this fashion, of course, is a value which includes errors in the parameterization, the satellite-derived cloud amount, the assumptions about surface albedo and humidity and the measurements of DSF. To convey the nature of this variable we therefore will refer to this variable as "effective optical thickness". Our goal is to obtain a representative set of values of effective optical thickness which can then be used in calculations of DSF for the entire domain while minimizing systematic errors. We therefore average optical depth from all measurements as a function of day of the year. Averaged optical depths were further interpolated and smoothed using a 30-day running mean. The result is essentially linear function for optical thickness of day of year.

Results

Figure A-2 shows the results of this operation for data from the NP station data set. Using an averaged "effective optical depth" measured DSF was reproduced with an RMS error 32 Wm^{-2}; the amount of explained variance is 91%. It is important to note that this is not an independent data set because the "effective optical thickness" was calculated from the same data. Obviously, if we hadn't averaged and smoothed the "effective optical thickness" and had computed one for each measurement, then the RMS error would be 0 and the explained variance 100%. In order to evaluate the procedure for an independent data set we computed the measured DSF at the site of the SHEBA experiment (October 1997 - August 1998) and at Barrow (January 1992-July 1993). For each of the sites surface measurements of DSF were averaged to daily values and compared to the closest grid cell in the PFLX data set. Figures A-3 and A-4 show the results for the SHEBA and Barrow sites. RMS errors for SHEBA are 34 Wm^{-2} with a mean error of less than 1 Wm^{-2} and an explained variance of 89%. Results for Barrow were similar with an RMS of 30 Wm^{-2}, a slightly larger mean error of 7 Wm^{-2} and an explained variance of 93%. These errors are in the same order of magnitude as can be achieved with parameterizations using surface observations. RMS errors in the order of 30 Wm^{-2} appear relatively large in light of the considerable sensitivities of sea ice

model results due to changes in surface fluxes. However, because systematic errors have largely been removed from the results by our procedure, we believe that random errors of this magnitude are of little consequence for sea ice model output.

Application

The above paragraphs served to describe and demonstrate the effectiveness of our approach to compute DSF. For the application in our model runs we altered the approach slightly. Rather than specifying a downwelling shortwave flux as an external forcing field, we compute DSF within the sea ice model using cloud fraction from the TOVS Path-P data set, NP-station derived "effective optical depth" and model calculated albedo as inputs. This offered several advantages with respect to the model configuration and allowed for the interaction of surface albedo with DSF. Because differences in the orientation of the grids used by the sea-ice model and for the retrieval of Path-P (> 60°N) data, several grid-cells of the model domain (< 60 °N) are not included. Cloud fractions for these areas were set to 0.5. Missing days (very few) in the cloud retrieval were replaced by interpolates in time.

Downwelling longwave fluxes (DLF)

Downwelling longwave fluxes were computed in a similar way. In keeping with the recommendations of Key and al. (1996), we selected the parameterization of Efimova (1961) and Jacobs (1978) for downwelling longwave fluxes because it performed best in their comparisons of parameterized clear (LW_{clr}) and cloudy (LW_{cld}) downwelling longwave fluxes with measurements from various ice and land-based stations (Equation 2):

$$L_{clr} = \sigma T_{air}^4 (0.746 + 0.0066 * e)$$
$$L_{Cld} = L_{clr}(1 + 026) * C \qquad (2)$$

where σ is the Stefan Bolzman constant, T_{air} the surface air temperature, e the vapor pressure and C the cloud fraction. A comparison of this parameterization using SHEBA data further supports the validity of this parameterization. As in the computation of DSF, cloud amounts are again taken from the TOVS Path-P data set and surface temperature from the IABP/POLES temperature set (Rigor et al. 2000). Water vapor pressure (e) was set to saturation. Figures A-5 show a comparison of parameterized fluxes with measured fluxes for the SHEBA site. Surface air temperatures in this case were taken from the 2-m measurements at the SHEBA tower. But because these measurements are used in the construction of the IAPB/POLES data set, there is little local difference. Cloud amounts are from meteorological surface observations a) and the TOVS Path-P data set b). Using TOVS cloud fractions and the original parameterization of Efimova and Jacobs (E&J) would have resulted in a slight positive bias of DLF during winter. Coefficients in Equation 2 were therefore readjusted to yield the unbiased results shown in figure A-5 b. RMS errors for the DLF are 12 Wm^{-2} and 15 Wm^{-2} for surface clouds versus. Path-P clouds respectively. Explained variance (R^2 *100) are 98% and 93%. In order to validate the DLF approach using an independent data set, PFLX DLF (using IABP/POLES temperatures as inputs, TOVS Path-P cloud) were compared to measurements near Barrow Alaska (Figure A-6). In comparison to the SHEBA site, RMS

errors were about 22 Wm^{-2} and the explained variance being only 85%. However, errors are still largely random with a mean error of less than 1 Wm^{-2}. The small systematic errors in this independent data set support the viability of computing DLF using our approach. The improvement in the annual cycle of DLF over the STANDARD forcing field can be seen in figure A-7

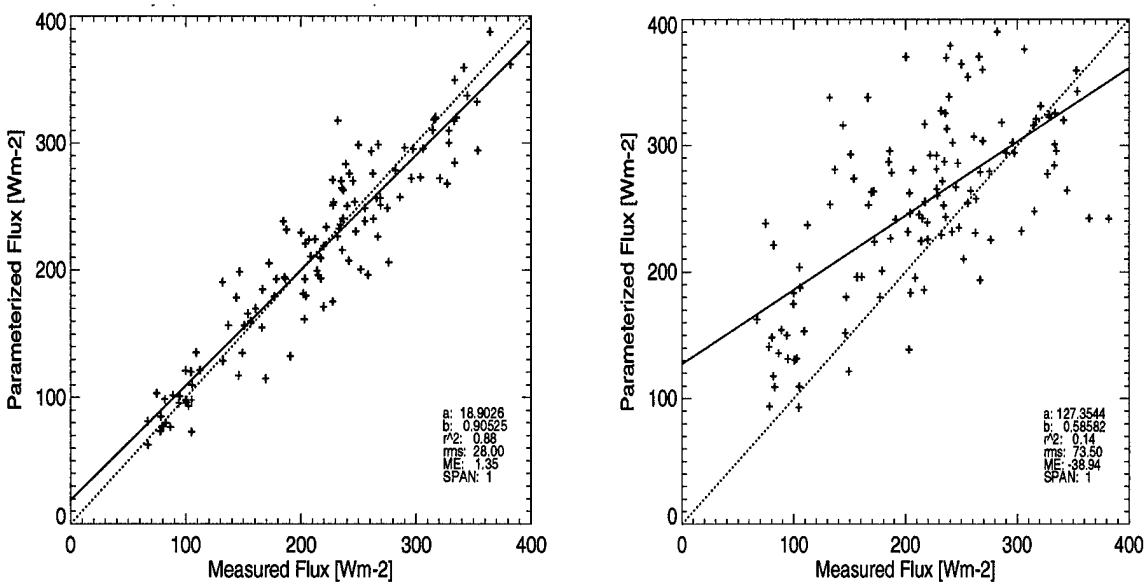

Figure A-1: Comparison of measured surface fluxes with those parameterized using observed cloud fraction and a random cloud fraction. Data are for the SHEBA site from May-August 1998. Cloud observations are from the meteorological observations, optical depth is inverted from measurements and averaged to mean monthly values (4 values for May-August). Using random clouds, the explained variance by the parameterization drops to 14% from 88%. This result indicates the importance of cloud fraction and the value of such relatively simple observations for the computation of DSF.

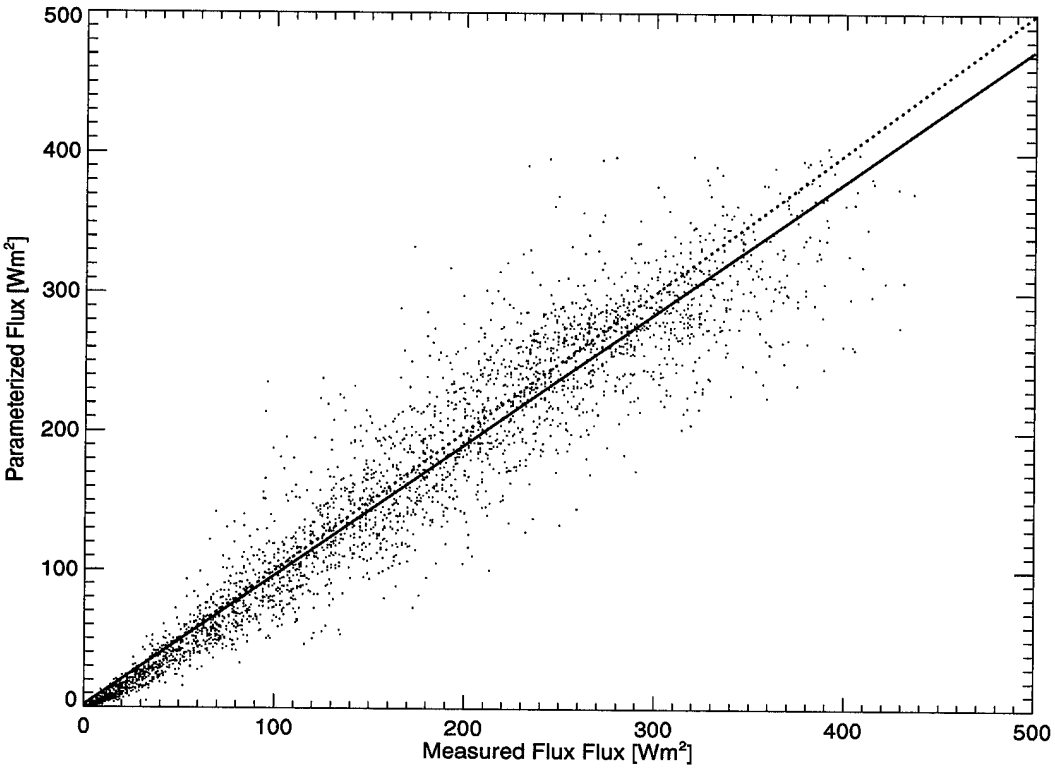

Figure A-2: Parameterized and measured downwelling shortwave flux at the ice surface using TOVS-derived cloud amount, averaged optical depths values inverted from measurements. Data are from the NP station data set from 1980 through 1991.

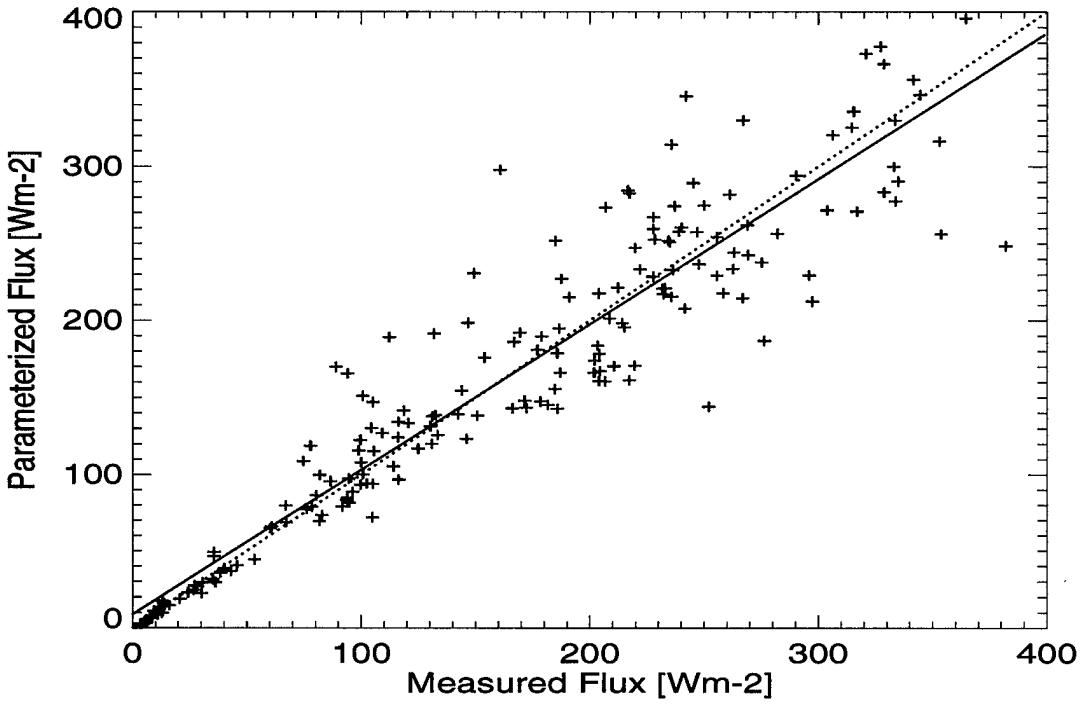

Figure A-3: Observed and Parameterized downwelling shortwave flux at the surface at the SHEBA site. Measured DSF are daily averaged observations from November 1997 through August 1998. Parameterized DSF is based on daily cloud fractions from the Path-P project, surface albedo averaged from the NP stations data set, and "effective cloud optical depth" also from the NP station data set.

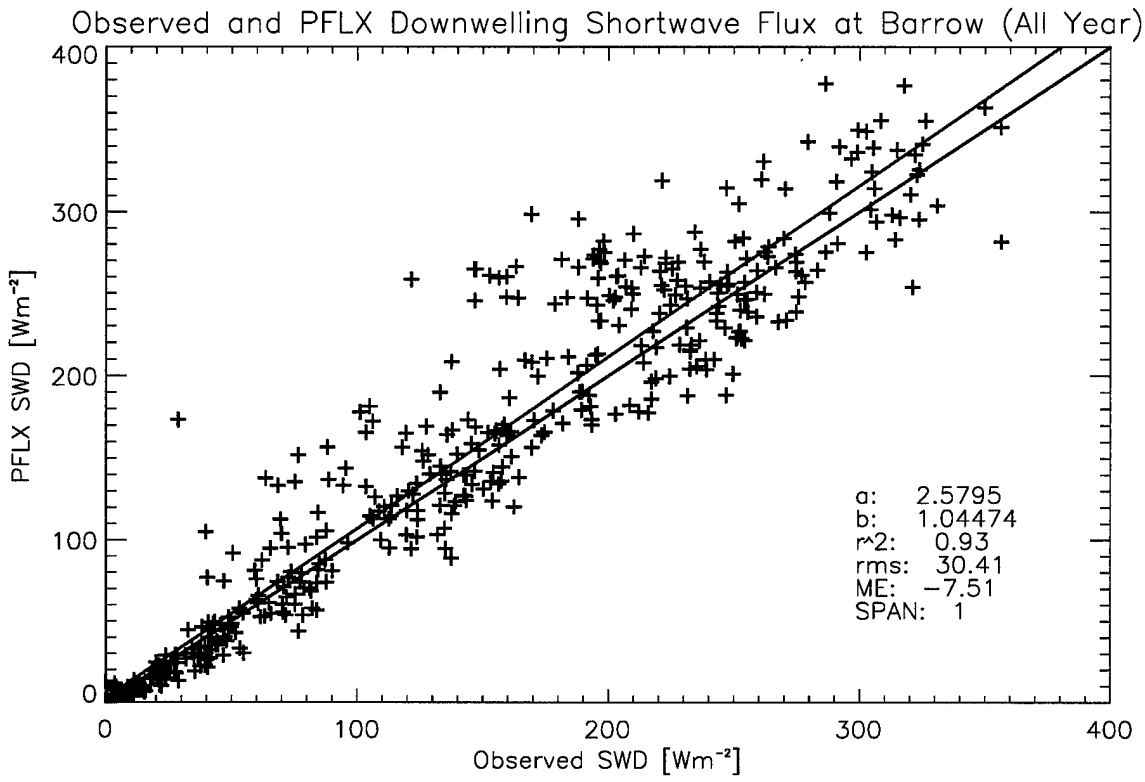

Figure A-4: Observed and Parameterized downwelling shortwave flux at the surface at the Barrow site. Measured DSF are daily averaged observations from January1992 through July 1993. Parameterized DSF (PFLX) is based on daily cloud fractions from the Path-P project, surface albedo averaged from the NP stations data set, and "effective cloud optical depth" also from the NP station data set.

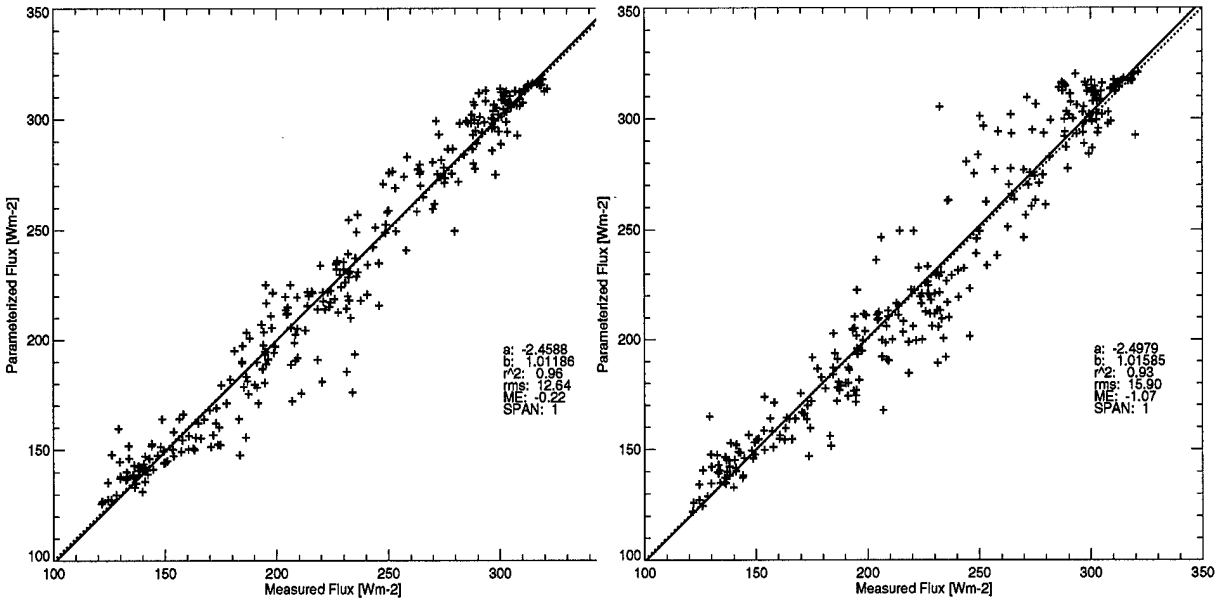

a) b)

Figure A-5: a,b. Measured and parameterized downwelling longwave flux at the surface (DLF) at the SHEBA site (November 1997 - August 1998). Input data for the parameterizations are surface temperatures measured at the SHEBA site, and surface observed (a) and TOVS-observed cloud fractions, respectively. Water vapor pressure was set to saturation with respect to ice.

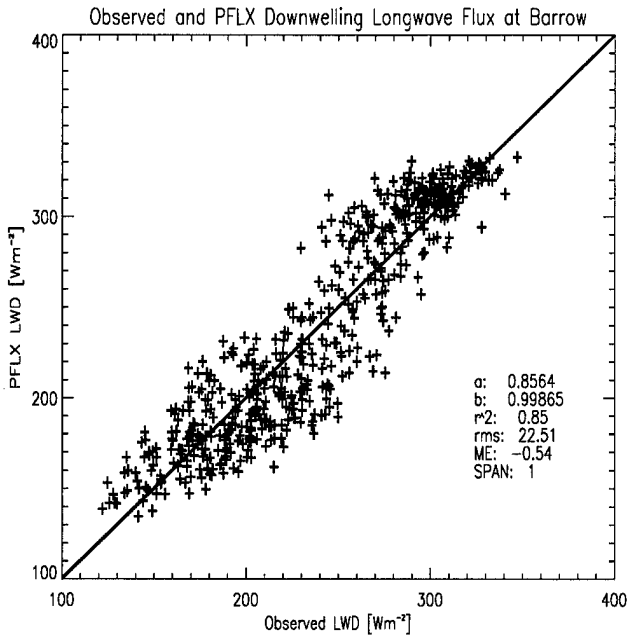

Figure A-6: Comparison of parameterized PFLX and measured downwelling longwave fluxes DLF at the Barrow site (January 1992 - July 1993). Input data for the parameterization are IABP/ POLES for temperature and TOVS Path-P.

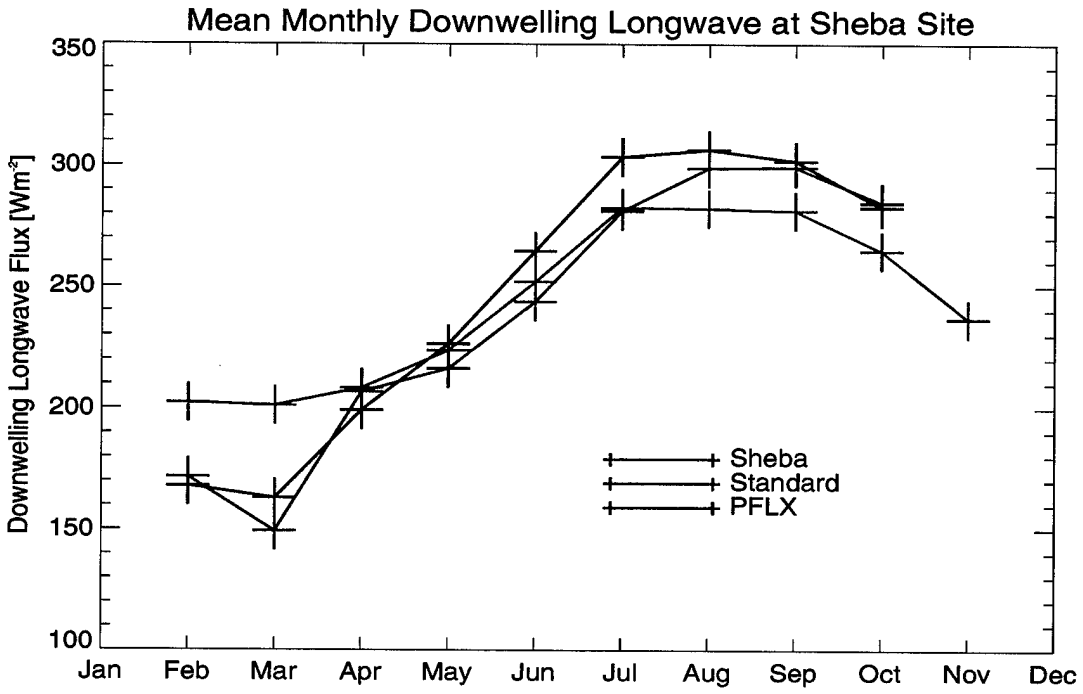

Figure A-7: Mean monthly downwelling longwave flux at the SHEBA site. Shown are measured fluxes (SHEBA), PFLX and STANDARD fluxes.

References

Armstrong, R. L. and M. J. Brodzik, 1995. An earth-gridded SSM/I data set for cryospheric studies and global change monitoring. Advances in Space Research 10:155-163.

Bitz, C, J. Fyfe and G. Flato. (in press). Sea ice response to wind forcing from AMIP models. Journal of Clmate, preprint at : http://www.atmos.washington.edu/~bits/bitz01.ps

Beesley, John A., 2001: Evaluation of NOGAPS Atmospheric Forcing for the PIPS Sea-Ice Model: Comparison with Observations in the Arctic. NIC Technical Report, 19 pp. [Available from National Ice Center, FB #4, 4251 Suitland Road, Washington, D.C., 20395.]

Efimova, N. A., 1961. On methods of calculating monthly values of net long-wave radiation. Meteor. Gidrol., 10, 28-33

Fischer, H. and P. Lemke, 1994. On the Required Accuracy of Atmospheric Forcing Fields for Driving Dynamic-Thermodynamic Sea ice Models. In: The Polar Oceans and Their Role in Shaping the Global Environment. Eds. O. M. Johannessen, R.D. Muench and J.E.Overland. Geophysical Monograph, 85. Agu, 373-381

Flato, G. M., and W. D. Hibler III. 1995. Ridging and strength in modeling the thickness distribution of Arctic sea ice. J. Geophys. Res., 100, 18,611-18,626.

Francis, J.A. and A.J. Schweiger, 2000: A new window to the Arctic, *Eos Trans., AGU, 81,* 77-78

Hibler, 1980. Modeling a variable thickness sea ice cover. Mon. Wea. Rev. 108, 1943-1973

Idso, S. B, and R. D. Jackson, 1969. Thermal radiation from the atmosphere. J. Geophys. Res., 74, 5397-5403.

Ip, C.F, 1993. Numerical Investigation of different rheologies on sea ice dynamics, Ph.D dissertation, 242pp., Thayer Sch. of Eng., Darthmouth, Coll., Hannover, N. H. 1993

Jacobs, J.D. 1978. Radiation climate of Broughon Island. Energy Budget Studies in Relation to Fast-Ice Breakup Processes in Davis Stratt. R. G. and J.D. Jacobs, Eds. , INSTAAR, University of Colorado, 105-120.

Kalnay, E., Kanamitsu, M. Kistler, R. Collins, W. Deaven, D. Gandin, L. Iredell, M. Saha, S. White, G. Woollen, J. Zhu, Y. Chelliah, M. Ebisuzaki, W. Higgins, W. Janowiak, J. Mo, KC. Ropelewski, C. Wang, J. Leetmaa, A. Reynolds, R. Jenne, Roy. Joseph, Dennis, 1996, The NCEP/NCAR 40-year reanalysis project. Bulletin-of-the- American-Meteorological-Society. March, 77, 437-471.

Key, J. R., R. A. Silcox, R. S. Stone, 1996: Evaluation of surface radiative flux parameterizations for use in sea ice models. J. Geophys. Res., 101(C2), 3839-3849.

Kwok, R., A. Schweiger, D. A. Rothrock, S. Pang, and C. Kottmeier, 1998: Sea ice motion form satellite passive microwave imagery assessed with ERS SAR and buoy motions, J. Geophys. Res., 103 (C4), 8191-8214.

Lemke, P. W. D. Hibler, G. Flato, M. Harder and M. Kreyscher, 1997. On the improvement of sea-ice models for climate simulations: the Sea Ice Model Intercomparison Project., Annals of

Glaciology, 25, 183-187.

Lindsay, R. W., 1998: Temporal variability of the energy balance of thick Arctic pack ice. J. Climate, 11, 313-331.

Maslanik, J.;Fowler, C., Key, J. R., Scambos, T, Hutschinson, T, and Emery, W. 1997. AVHRR based Polar Pathfinder products for modeling applications. Annals of Glaciology, Vol. 25, 1997, p338-92

Maykut, G. A., and N. Untersteiner, 1971: Some results from a time-dependent thermodynamic model of sea ice. J. Geophys. Res., 76. 1550–1575.

Parkinson, C., L., and W., M., Washington, 1979: A large-scale numerical model of sea ice. *J. Geophys. Res.*, **84**, 311-337.

Persson, P. Ola G., C. W. Fairall, E. Andreas, P. Guest and D. Perovich, 2000: Measurements near the Atmospheric Surface Flux Group tower at SHEBA Part I: Site description, data processing, and accuracy estimates, J. Geophys. Res.

Persson, P. Ola G., C. W. Fairall, E. Andreas, and P. Guest, 2000: Measurements nearthe Atmospheric Surface Flux Group tower at SHEBA Part II: Near-surface conditions and surface energy budget, J. Geophys. Res.

Rigor, I., R. Colony, and S. Martin, 2000: Variations in Surface Air Temperature Observations in the Arctic, 1979 - 1997. J. Climate, 13, 896–914.

Rothrock, D. A., J. Zhang, and Y.Yu. (submitted). The Arctic Ice Thickness Anomaly of the 1990s- A Consistent View from Observations and Models. Journal of Geophysical Research (submitted Oct 2001)

Rothrock, D., A. and J. Zhang, 1996. Surface Downwelling Radiatiative Fluxes: Model Sensitivities and Data Accuracies. In proceedings of the AMS Workshop on Polar Processes in Global Climate, Cancun, 13-15 November 1996.

Schweiger, A. J., R. W. Lindsay, J. R. Key, and J. A. Francis. 1999: Arctic clouds in multiyear satellite data sets. *Geophys. Res. Lett. 26(13),* 1845-48.

Schweiger, A.J., R.W. Lindsay, J.A. Francis, J. Key, J. Intrieri, and M. Shupe, (in press): Validation of TOVS Path-P data during SHEBA. *J. Geophys. Res.,* Preprint at: http:// psc.apl.washington.edu/pathp/Documents/pathpjgr.pdf

Serreze, M.C., J.R. Key, J.E.Box, J. A. Maslanik and K. Steffen. 1998. A new climatology of global radiation for the Arctic and Comparisons with NCE-NCAR Reanalysis and ISCCP-C2 Fields. Journal of Climate, Vol.11, 121-136)

Shine, K. P. , 1984: Parameterization of the shortwave flux over high albedo surfaces as a function of cloud thickness and surface albedo. J. R. Meteor. Soc., 110, 747-764.

Thorndike A.S., D.A. Rothrock, G.A. Maykut, and R. Colony. 1975. The thickness distribution of sea ice. J. Geophys. Res.,80, 4501-4513.

Winton, M.A., 2000. A reformulated three-layer sea-ice model. J. Atmos. Ocean. Tech., 17, 525-531,2000.

Zhang, J. 1993. A high-resolution ice-ocean model with imbedded mixed layer. Ph.D. thesis, Darmouth College, 229 pp. [Available from Dartmouth Collaged, Hanover, NH 03755]

Zhang, J. and D. A. Rothrock. 2001. A thickness and enthalpy distribution sea-ice model, J. Phys. Oceanogra., 31, 2986-3001.

Zhang, J. and D. Rothrock, 2000: Modeling Arctic sea ice with an efficient plastic solution. J. Geophys. Res., 105(C2), 3325-3338.

Zhang, J., and W.D. Hibler, 1997, On an efficient numerical method for modeling sea ice dynamics, J. Geophys. Res., 102, 8691-8702.

Zhang, J., D. Thomas, D. A. Rothrock, R. W. Lindsay, Y. Yu, and R. Kwok (submitted): Assimilation of ice motion observations and comparisons with submarine ice thickness data. J. Geophys. Res., submitted.

Zhang, J., W.D. Hibler III, M. Steele, and D.A. Rothrock, 1998: Arctic ice-ocean modeling with and without climate restoring. J. Phys. Oceanogr., 28, 191–217.

Zillman, J. W. , 1972. A study of some aspects of the radiation and heat budgets of the southern hemisphere oceans, Meteorol. Stud. 26, 562 pp. Bur. Of Meteorol. Dep. Of the Interiod, Canberra, Australia.